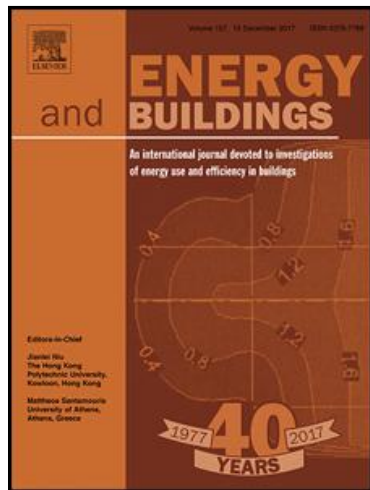


# Accepted Manuscript

Climatic performance of urban textures: analysis tools for a Mediterranean urban context

Agnese Salvati , Paolo Monti , Helena Coch Roura , Carlo Cecere

PII: S0378-7788(18)30529-2  
DOI: <https://doi.org/10.1016/j.enbuild.2018.12.024>  
Reference: ENB 8953



To appear in: *Energy & Buildings*

Received date: 13 February 2018  
Revised date: 4 October 2018  
Accepted date: 22 December 2018

Please cite this article as: Agnese Salvati , Paolo Monti , Helena Coch Roura , Carlo Cecere , Climatic performance of urban textures: analysis tools for a Mediterranean urban context, *Energy & Buildings* (2019), doi: <https://doi.org/10.1016/j.enbuild.2018.12.024>

This is a PDF file of an unedited manuscript that has been accepted for publication. As a service to our customers we are providing this early version of the manuscript. The manuscript will undergo copyediting, typesetting, and review of the resulting proof before it is published in its final form. Please note that during the production process errors may be discovered which could affect the content, and all legal disclaimers that apply to the journal pertain.

**Highlights**

- Urban morphology has the highest impact on UHI intensity in Mediterranean climate
- UHI intensity can be estimated based on three descriptors of urban morphology
- Climate performance of urban textures varies in summer time and winter time
- Compactness and vertical density are key morphological features for UHI assessment

# Climatic performance of urban textures: analysis tools for a Mediterranean urban context

Agnese Salvati<sup>ab\*</sup>, Paolo Monti<sup>a</sup>, Helena Coch Roura<sup>b</sup>, Carlo Cecere<sup>a</sup>

<sup>a</sup>Sapienza University of Rome, DICEA Department, SOS\_UrbanLab, Via Eudossiana 18, 00184 Rome, Italy

<sup>b</sup>Polytechnic University of Catalunya, School of Architecture, AiEM, Av. Diagonal, 649, 08028 Barcelona, Spain

\*Corresponding author: agnese.salvati@uniroma1.it

## Abstract:

Urban heat island effect is almost always neglected in building energy simulations, due to difficulties in obtaining site-specific climate data with a district-scale resolution. This study aims at filling this gap for the Mediterranean urban context, presenting a set of tools to estimate the climatic performance of urban fabric at the local scale.

The results are based on climatic analysis conducted in Rome (Italy) and Barcelona (Spain) with the Urban Weather Generator (UWG) model, validated using temperature measurements taken in urban meteorological stations. Parametric analysis of the UHI intensity were performed considering five key variables: urban morphology, vegetation cover, anthropogenic heat from buildings, anthropogenic heat from traffic and albedo. The results show that the variability of urban morphology has the major impact on urban temperature. Two robust relationships between three morphology descriptors of urban fabric and UHI intensity were established applying multiple regression analysis. Such relationships indicate that both the horizontal and the vertical density of buildings play a major role on the temperature increase in urban areas. Easy-to-use graphical tools have been provided to compare the climate performance of different urban textures and to estimate the average UHI intensity variability in Mediterranean cities.

## 1. Introduction

Heat vulnerability in urban areas is one of the most concerning impacts of climate change in hot climates [1].

The increase in frequency of strong heat waves observed in Europe and the Mediterranean region since

2000 has caused severe impacts on population's health and comfort [2–4]. Mediterranean urban

environments are particularly prone to temperature increase because of some inherent characteristics, such

as lack of humidity, scarce vegetation, high building density and presence of anthropogenic heat sources,

which are responsible of the so-called 'Urban Heat Island' (UHI) effect. In this context, the combination of

heat waves and UHI causes a significant increase of buildings cooling demand and electricity consumption

[5–7], which already accounts for the biggest share of the carbon emission related to the building stock [8].

For this reason, the impact of UHI intensity on building energy consumption in urban environments should be

carefully considered to effectively meet the target of CO<sub>2</sub> emission reduction set for the next decades [9].

The increase of temperature in urban areas is due to anthropogenic sources of heat, such as the buildings'

cooling and heating systems, and to mechanical and thermal phenomena determined by the interaction of

urban surfaces with the lower layers of atmosphere. The impact of built environments on air temperature

increase has been computed coupling mesoscale meteorological models with building energy models [10–

13]; these studies showed that the waste heat from buildings' systems and the albedo of surfaces play a

fundamental role on the increase of urban temperature. On the other way round, the increase of urban

temperature affects the energy performance of buildings in urban areas. Recently, new methodologies for

predicting buildings energy loads at a district and an urban scale have been proposed [14–19]. Most of these

take into consideration the impact of microclimatic modifications produced by built environments, such as the

UHI effect. The results indicate that the energy performance of buildings is influenced by the urban form and

building density, which modify both urban temperature and indoor solar gains [20–25].

The influence of urban geometry on UHI intensity has been investigated in several experimental and

numerical studies [26–30]. However, the findings of these kind of studies are not of help to obtain urban

climate data with a local scale resolution, because they are normally based on a sole geometrical parameter,

namely the canyon "aspect ratio" - the ratio of the buildings height (H) to the width (W) of the road - or the

canyon "Sky View Factor" (SVF). These dimensionless parameters alone are not fully adequate to

characterise the three-dimensional features of different urban morphologies, because to same values of SVF

or H/W ratios, different urban configurations may exist (figure 1). Other studies on urban morphology

demonstrated in fact that more than one metric is needed to understand the urban typologies associated to a

certain density [25,31,32]. The dimensions and the shape of buildings are fundamental variables to

understand the interaction between atmosphere and urban surfaces that determines the local urban climate; therefore, a more suitable set of morphology descriptors should be identified to quantitatively assess the climate performance of urban textures.

This work aims at filling this research gap for the Mediterranean context, introducing a set of analytical and graphical tools capable of predicting the climatic performance of different urban textures based on relevant morphological descriptors. This is aimed at providing easy-to-use analysis tools for designers and planners to perform urban climate analyses at the local scale and to adjust weather files for building energy modelling so as to include the UHI effect in urban areas. To this aim, the objective of this study is threefold. First, to validate the climate model ‘Urban Weather Generator’ in the Mediterranean context. Second, to identify quantitative relationships between a set of descriptors of urban morphology and the estimated UHI intensity during winter season and summer season at the local scale. Third, to provide graphical tools to compare easily the climatic performance of different urban textures in a Mediterranean urban context.

### 1.1 Background

The UHI and its impact on building energy performance have been widely investigated in previous studies [33–35]. In the Mediterranean zone, the maximum UHI intensity has been found to vary between 2°C and 10°C or even more [34,36]. Many experimental and numerical studies have been carried out in Rome and Barcelona, two of the largest urban areas of the Mediterranean basin. The results showed a variation of the average maximum UHI intensity between 2°C and 5°C [37–41], determining an increase up to 57% of the cooling demand of residential buildings [37,42,43]. The impact on non-domestic buildings (e.g. university) is instead around 10% in this climate [44,45]. The negative impact of UHI intensity on cooling loads and cooling potential of natural ventilation has been highlighted also in colder climates, such as in London, UK, or in Basel, Switzerland [6,46,47].

#### Limitations of Urban Canyon parametrisation:

**A bidimensional parametrisation** does not consider:

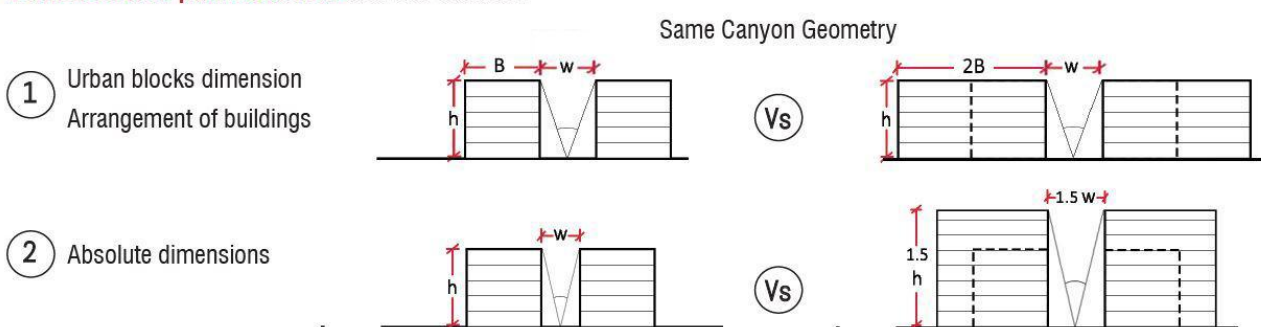


Figure 1: Limitations of dimensionless parameters in describing urban morphology (2-column fitting image)

Other studies on the UHI highlighted that the spatial distribution of urban temperature is not uniform, the latter being dependent mainly on the density of buildings [48,49]. This fact can be explained by considering three typical phenomena that characterize densely built environments: 1) solar radiation absorption is increased because of multiple reflections between the surfaces of the urban canyons [50], 2) turbulent sensible heat transfer out of the canyon is reduced due to the building proximity that decreases wind speed [51,52] and 3) long-wave radiation loss from within the canyon is reduced due to the screening by the flanking buildings [28,46].

An analytical relationship between urban geometry and UHI intensity was firstly presented by Oke [53], who found a logarithmic relationship between the increase of UHI intensity and the increase of the canyon aspect ratio. Many other empirical relationships have also been identified for different cities and climates, as presented in the reviews by Unger [50,54–56]; the results are however quite inconsistent and hardly comparable, due to the different climates, urban characteristics and observational periods.

Oke also proposed a practical methodology to link urban climatology analysis to urban planning, introducing the concept of ‘Urban Climate Zones’ (UCZ) [57], successively evolved in ‘Local Climate Zones’ (LCZ) [49]. The LCZ method divides the urban fabric into homogeneous categories in terms of built types, land cover types and land use, with the aim of predicting intra-urban temperature patterns and UHI intensities. Built types are classified in ten categories, comprehensive of compact, open and sparse developments with different building height (high-rise, midrise, low-rise). Recently, effective methodologies to produce LCZ maps using data from remote sensing images and GIS databases have also been presented [58–60]. However, the classification of built types in the LCZ method has limitations regarding the possibility to cover the many building configurations typically observed in real urban environments [61].

To estimate the UHI intensity at the district scale, many urban energy balance models (UEB) [62,63] and computational fluid dynamic models (CFD) have also been proposed. UEBs simulate the urban energy fluxes at the local scale based on the building-air volume balance defined by Oke [64]. They use incoming shortwave and long wave radiative fluxes, air temperature, specific humidity, wind components and anthropogenic heat flux as forcing conditions and model the outgoing radiative fluxes, turbulent sensible heat flux, turbulent latent heat flux and net heat storage flux of a given urban system. In these models, urban morphology is described using different sets of parameters, varying from model to model [62].

CFD models can be much more accurate than UEBs, because they solve the governing equation of fluid motion with high spatial resolution [26]. Many studies on the impact of urban morphology on urban

microclimate have been developed with CFDs [65–68]. Procedures for coupling building energy models with CFD models or urban canopy parametrizations have also been proposed to account for the reciprocal interaction between indoors and outdoors in urban contexts [12,26,69–72].

UEB and CFD models thus represent an important progress for climate analysis in urban areas. Nevertheless, they have had poor application in urban planning and building design. CFD tools and coupled models can provide high-resolutions microclimate data for short times, but presuppose expert knowledge and suffer from very long calculation times, which limit their adoption especially for analysis at the district scale [73]. UEB models are less sophisticated but they also need a basic knowledge of urban climate physics to be used properly; also, their application is limited by the fact that the output data - i.e. urban energy fluxes or surface temperatures - are not directly usable to perform building energy analysis. In fact, this lack of communication between tools, disciplines and expertise remains the main limitation for an integrated assessment of the building energy performance in urban environment.

A step forward was done with the development of the 'Urban Weather Generator' (UWG) [74]. UWG is based on the UEB model 'Town Energy Balance' [63,75], including a detailed Building Energy Model [76,77] to account for the reciprocal interaction between buildings energy performance and urban climate (i.e. heat transfer through building fabric and waste heat from heating, ventilation and air conditioning systems). UWG uses hourly data measured at rural meteorological stations as forcing conditions to calculate urban energy fluxes and to generate urban weather files that capture the UHI intensity for a reference urban area. The model consists of four calculation components: the "Rural Station Model" (RSM), the "Vertical Diffusion Model" (VDM), the "Urban Boundary-layer model" (UBL) and the "Urban Canopy and Building Energy Model" (UC-BEM)". The model workflow is as follow: the input weather data are used by the RSM to calculate the rural sensible heat flux, which is used by the VDM to calculate the vertical profile of air temperature above the rural weather station. These data, along with the urban sensible heat flux calculated by the UC-BEM, are used by the UBL to calculate air temperature above the urban canopy layer. The UC-BEM calculates urban sensible heat flux and urban canyon air temperature and humidity from radiation and precipitation data, air velocity and humidity measured at the weather station and from the air temperature calculated by the UBL. The equations and interrelations between models are described in detail in the relevant publication [74]. The main advantages of this model with respect to others are: 1) short computation time, 2) use of hourly weather files to force the calculation, which allows for an assessment of the hourly variability of UHI intensity over a year and 3) direct usability of the output weather files to run building energy performance simulations with EnergyPlus. To perform simulations with UWG, two files are needed: a rural weather file and an XML file

which describes all the features of the urban area that affect the phenomenon, urban morphology included [74]. The first version of the model (V 1.0) has been validated in Boston, Basel and Toulouse, showing an average Root Mean Squared Error (RMSE) of about 1K [74,78]. Updated versions of the model have recently been validated in Singapore and Abu Dhabi [79,80].

UWG appears to be particularly suitable for comparative analysis of the climatic performance of the urban textures as it considers a morphology parameterization based on three independent descriptors: the “site coverage ratio”, the “average building height” in the area and the “façade to site ratio”. This set of parameters provides quantitative details on building density and qualitative information on the urban typology (this point is discussed in detail in section 4). Results from this model could thus be used for quantitative comparisons of the climatic performance of different urban textures as well as to derive qualitative insights into the relationship between urban morphology and climate performance at the local scale.

## **2. Materials and method**

In this study, the climatic performance of the urban texture (from this point on considered as a portion of urban fabric homogeneous for morphology) is defined as the average UHI intensity occurring during summer season and winter season. UWG model has been used to assess the variability of the UHI intensity at the local scale, considering different urban textures of Rome and Barcelona as case studies. The local scale is defined as an urban area of diameter around  $10^3$  m with similar types of surface cover, land use and building density [57], which thus corresponds to the assessment of UHI intensity in different urban textures.

UWG has been validated using air temperature measurements from urban meteorological stations located in Rome and Barcelona, two large urban areas representative of the typical Mediterranean climate (both cities are “Csa – Hot-Summer Mediterranean climate” in Köppen-Geiger climate classification). A parametric analysis of UHI variability according to different urban variables has been carried out considering specific characteristics of the two cities. Quantitative relationships between three descriptors of urban morphology and the estimated climatic performance at the local scale are obtained applying multiple regression analysis.

### **2.1. Survey cities and validation of UWG model**

Rome and Barcelona are located at very close latitude (table 2). Previous meteorological studies on the cities showed that both Rome [81–83] and Barcelona [84] are characterized by mild synoptic wind speeds and that the sea-breeze is usually predominant for most part of the year, with a pronounced daily cycle. They

show similar trends of the monthly average temperature (figure 2), even though the thermoregulatory effect of the sea tends to lower the amplitude of the temperature range in Barcelona.

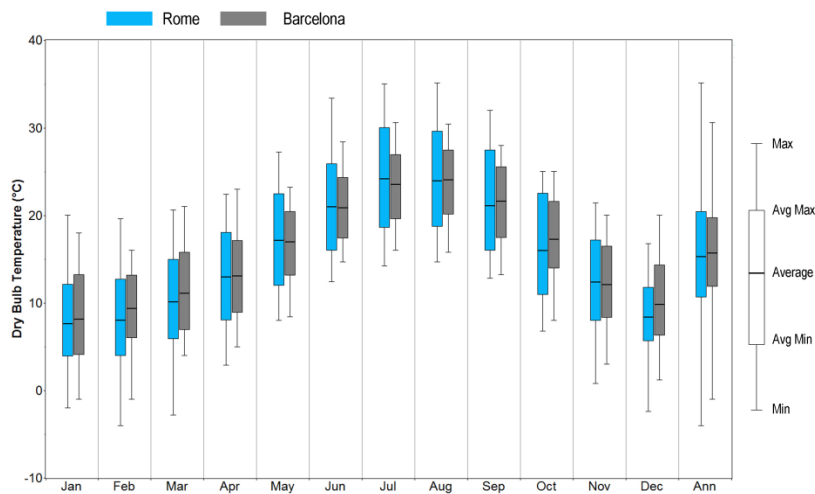


Figure 2 Comparison between the monthly average, minimum and maximum temperature in Rome (blue) and Barcelona (grey) based on historical series of data from 'El Prat' airport weather station for Barcelona (period 1981-2010) and Ciampino Airport weather station for Rome (period 1951-1970) - (1.5 column fitting image)

### 2.1.1. Model validation with field data

The validation of UWG model v 1.0 is based on one-year data of hourly air temperatures collected at two weather stations located in the city centre of Rome and Barcelona (figure 3). The rural weather files used as input to run the simulations refer to cities airport weather stations, namely Ciampino Airport (Rome) and El Prat Airport (Barcelona).

UWG uses hourly data of temperature, radiation, humidity and wind speed from the rural weather file to calculate the hourly average urban temperature, but it does not calculate wind speed and direction in the urban area. For this reason, the model validation is based only on temperature data. Nevertheless, this important limitation must be taken into consideration when performing urban building energy analyses with UWG weather files.

The simulation period was one year for both cities. The model accuracy has been assessed comparing monthly average temperatures and diurnal cycles of air temperature estimated by UWG and measured at the urban weather stations. The discussion of the model performance is presented separately for summer season and winter season.

### 2.1.2. Data sources and model set-up

The hourly temperature data recorded at the airports weather stations were taken from the website 'Weather Underground' [85,86], while the Meteorological service of Catalonia (METEOCAT) and the Regional

Environmental Protection Agency (ARPA LAZIO) provided hourly temperature data for the two urban weather stations in Barcelona and Rome, respectively. Both weather stations are located in the old town centre of the cities, in very similar contexts in terms of building density and vegetation cover and land use characterised by a mix of residential buildings, public facilities and offices.

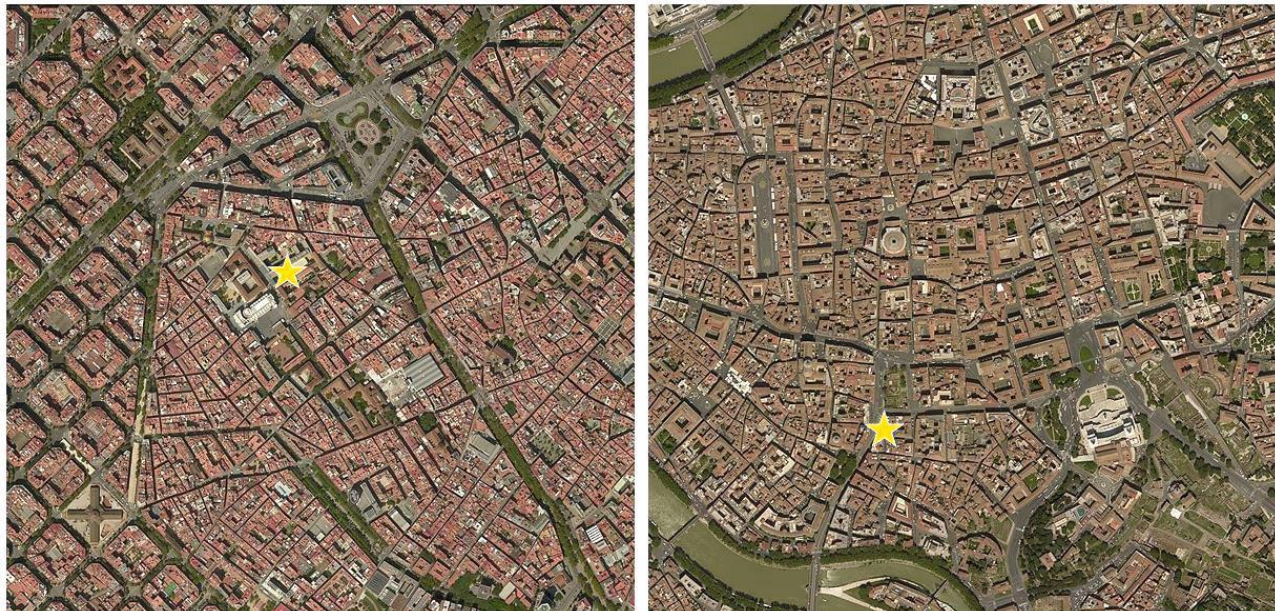


*Figure 3 Location of the urban weather stations in Raval (Barcelona) on the left and in Via Arenula (Rome) on the right. The yellow stars indicate the positions of the weather stations - (2 column fitting image)*

*Table 1: Urban weather station and sensors location*

Weather Station	Dist. from Airport (Km)	Dist. from the Sea (Km)	Height (m)	sensor	Position	Reference Year
Raval, Barcelona	13	1,3	33 a.s.l.		Rooftop	2013
Via Arenula, Rome	13	24	31 a.s.l.		Street level	2003



Figure 4 The yellow areas represent the footprints of Raval weather station (left) and Via Arenula weather station (right). - (2 column fitting image)

The two weather stations differ in the position of the temperature sensors: the one in Barcelona is located on the top of a building while the one in Rome is at 2 m above ground level. Therefore, the two stations have also different footprints [87,88]. Since the temperature sensor in Rome was placed near the ground level, where buildings significantly modify wind directions, an area of about 500m radius centred in the station has been used as footprint (right panel in figure 4). Conversely, at Raval, only the downwind portion of the 500m radius area around the station has been considered as footprint, considering that North-West and South-Southwest are the main wind directions both in winter and in summer (left panel in figure 4). Each footprint has been used as source area for the calculation of the input parameters for UGW simulations. Table 2 lists the sources and the values of the main parameters used for the validation runs. More information on the calculation of UWG input parameters can be found also in a previous work [89].

Table 2: Input parameters for UWG validation

	Raval (Barcelona)	Via Arenula (Rome)	Data source and reference studies
<b>Reference Site</b>			
Latitude [°]	41.4	41.47	
Longitude [°]	2.2	12.34	
<b>Urban Area</b>			
Average Building height [m]	16.7	19.9	
Site coverage ratio [m <sup>2</sup> /m <sup>2</sup> ]	0.63	0.49	GIS data and CAD models
Façade-to-site ratio [m <sup>2</sup> /m <sup>2</sup> ]	2.19	1.44	
Tree coverage [%]	8.0	7.0	Aerial images from Google Earth®.
sensible anthropogenic heat	8.0	8.0	Pigeon et al [90]

[W/m<sup>2</sup>]**Building**

Daytime cooling set point [°C]	26	26	Zangheri et al. [91]
Nighttime cooling set point [°C]	35	35	The night time cooling set point set to 35 °C means absence of air conditioning
Daytime heating set point [°C]	20	20	
Nighttime heating set point [°C]	20	20	
<b>Elements</b>			
Wall albedo [-]	0.25	0.25	Site surveys and literature [74,92]
Wall materials and thickness	Brick, plaster - 43 cm	Brick, plaster – 43 cm	Estimated considering a typical masonry construction with low insulation
Roof albedo [-]	0.25	0.25	
Roof materials and thickness	Hollow-brick slab, screed, insulation, tiles, 38cm	Hollow-brick slab, screed, insulation, tiles, 38cm	
Road albedo [-]	0.08	0.08	Site surveys and literature [74,92]
<b>Rural reference</b>			
Albedo [-]	0.25	0.15	Areal images and literature [74,92]
Emissivity [-]	0.92	0.96	Bueno et al. [84]
Vegetation coverage [%]	20	48	Areal images from Google Earth®.

**2.2. Baseline model and parametric analyses of UHI intensity**

A parametric analysis of the UHI intensity variability has been performed with UWG to highlight what characteristic of the urban fabric affects more the UHI intensity in the two Mediterranean cities. The parametric analysis aims at assessing the range of variability of UHI intensity considering real characteristics of the urban fabric of Rome and Barcelona. For this reason, 10 urban textures (figure 5) have been chosen as case studies to calculate the average, maximum and minimum values of the most important variables of UHI. The following key variables were considered: urban morphology, vegetation cover, anthropogenic heat from traffic, waste heat from cooling systems and surface albedo. The corresponding UWG parameters are reported in table 3. More details on the calculation of the parameters are reported in the Appendix A.

Table 3: Definition of the UWG parameters used to perform the parametric analysis of UHI intensity variability

Variable	UWG Parameter	Definition
Urban Morphology	Average Building height - ( $h_{bld}$ ): Site coverage ratio - ( $\rho_{urb}$ ): Façade-to-site Ratio ( $VH_{urb}$ ):	average building height normalized by building footprint [m] ratio of the building footprint to the site area [-] ratio of the vertical surface area (walls) to the site area [-]
Vegetation Cover	Tree coverage:	ratio of the tree coverage in the urban area to the site area [%]
Anthropogenic heat from traffic	Sensible heat flux from traffic:	amount of heat released to the urban canyon as sensible heat from traffic (not from buildings) [W/m <sup>2</sup> ]
Waste heat from cooling systems	Daytime Cooling Setpoint:	indoor setpoint for mechanical cooling system during the day [°C]
Surfaces albedo	Wall albedo Roof Albedo Road Albedo	Ratio of reflected radiation from the surface (wall, roof, road) to incident radiation upon it

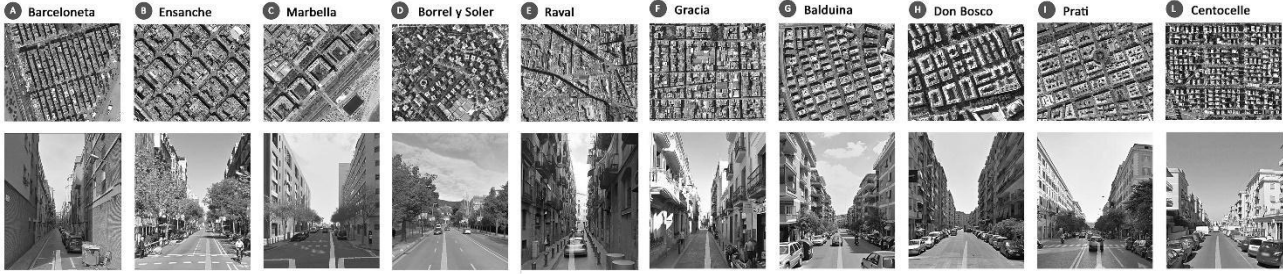


Figure 5 Urban textures of Rome and Barcelona used as case studies for the parametric analysis of UHI intensity - (2 column fitting image)

Table 4: Input values for the parametric analysis of UHI intensity with UWG. The values for the baseline model correspond to the average values among the 10 case studies.

	Max value	Min Value	Baseline Model
<b>Reference Site</b>			
Latitude [°]	-	-	41.47
Longitude [°]	-	-	12.34
<b>Urban Area</b>			
Average Building height [°]	25.5	11.6	19.5
Site coverage ratio [--]	0.8	0.2	0.49
Façade-to-site ratio [--]	2.23	0.63	1.43
Tree coverage [%]	28	5	12.0
sensible anthropogenic heat [W/m <sup>2</sup> ]	30	3	8.0
<b>Building</b>			
Daytime cooling set point [°C]	35	22	26
Night-time cooling set point [°C]	-	-	35
Daytime heating set point [°C]	-	-	20
Night-time heating set point [°C]	-	-	20
<b>Elements</b>			
Wall albedo	0.5	0.2	0.35
Roof albedo	0.35	0.1	0.25
Road albedo	0.2	0.04	0.08
<b>Rural reference</b>			
Albedo		0.15	
Emissivity		0.96	
Vegetation coverage [%]		48	

The sample of textures is representative of typical urban patterns of Mediterranean cities corresponding to different ages of development: from compact medieval structures to wide orthogonal networks typical of the Nineteenth century up to contemporary urban sprawl layouts [93,94]. The average values among the 10 case studies were used to define a ‘Baseline model’ for the Mediterranean context (table 5).

The parametric analysis of UHI intensity was performed testing the maximum and minimum values of each variable while maintaining all the other parameters to the values of the baseline model. To obtain comparable results, the rural weather file of Rome-Ciampino airport was used as input in all the simulations. The differences between the average maximum and minimum UHI intensity determined by the variability of each parameter were compared between each other and against the baseline model results (figure 7).

The variability of UHI intensity in different urban morphologies was analysed in more detail, performing one simulation for every set of morphology parameters corresponding to each of the 10 case studies, keeping constant all the other parameters to the baseline model.

### **2.3. Regression-based analysis**

Quantitative relationships between the three morphological parameters used by UWG and the estimated UHI intensity have been established applying multiple linear regression analysis, considering the average UHI intensity as dependent variable and the three morphological parameters as independent variables. The input data for the regression analysis consists of 108 simulation results, obtained fixing all the parameters to the baseline model except for the morphological ones, which varied according to defined ranges. The range of variability of each parameter was chosen in relation to the maximum and minimum values observed in the 10 sample textures. This was intended to include any possible urban configuration within the typical urban typologies of the Mediterranean context. Two different analyses were performed for the average summer and winter UHI intensity. The results from this wider set of simulations were used also to develop graphical tools for the analysis of the climate performance of urban textures in the Mediterranean context.

## **3. Results**

### **3.1 Accuracy of UWG predictions in the Mediterranean context**

The comparisons between the daily cycle of air temperature on the hottest and coldest months of the year as measured at the two urban weather stations and calculated by UWG are depicted in figure 6. The Coordinated Universal time (UTC) is used in the graphs; the local time zone is UTC+1 in winter and UTC+2 in summer. The results show that UWG captures reasonably well the average daily trends of air temperature in both cities. However, the model provides more accurate night-time predictions than the daytime ones for both cases, as already found in other studies [79].

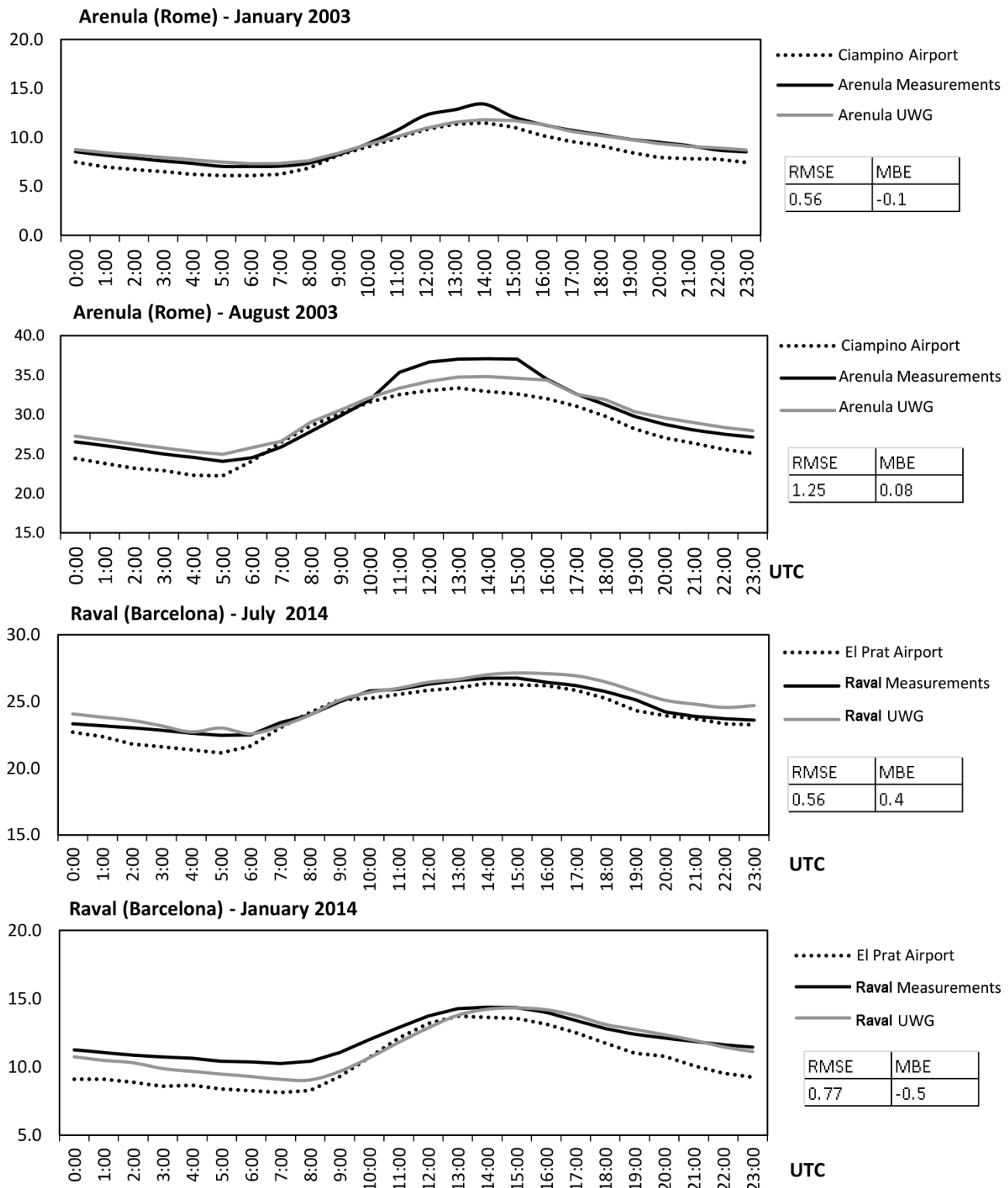


Figure 6 Comparison of the average daily profiles of air temperature calculated by UWG and measured at Via Arenula weather station (Rome) and Raval weather station (Barcelona). The dotted line represents the air temperature measured at the airport weather stations of the two cities, used as input for the simulations. - (2 column fitting image)

During daytime, the model underestimates the temperature for Rome (via Arenula) and overestimates those for Barcelona (Raval). The largest discrepancy between measurements and estimations regards Via Arenula between 12:00 and 15:00 UTC, when UWG underestimates urban temperature both in January and August.

With regard to Barcelona, the comparison between measurements and predictions shows that UWG tends to overestimate urban temperature in summer (Mean Bias Error = +0.4).

These inaccuracies could be explained by the different location of the urban temperature sensor, which was located at the street level at Arenula station and at the roof level at Raval station; this means that they measured the air temperature of different layers of atmosphere, namely the canopy layer in Rome (Via Arenula) and the roughness sub-layer in Barcelona (Raval). The fact that UWG is less accurate on daytime estimations is thus not surprising, because the diurnal cycle of air temperature in the two layers of atmosphere is significantly different [37,51,95], while the model only calculates an average value of the urban canyon temperature. It is in fact known that a vertical gradient exists in the urban canyon air temperature, which can be substantially warmer near ground level than roof level due to a combination of radiative and convective phenomena such as radiative trapping and wind obstruction [52,96–98]. This difference was clearly detected in a previous study on the experimental assessment of the UHI intensity in Barcelona, when a temperature difference of about 2°C was found during daytime in summer between the street level (higher temperature) and the roof level [37]. So, the temperature overestimation for Raval during summertime is probably due to an underestimation of convective effects by UWG, such as of the beneficial influence of sea breeze on temperatures at roof level, while the underestimation of air temperature for Arenula is probably due to an underestimation of the effect of radiative trapping in the canyon. These inaccuracies were predictable because UWG does not calculate the vertical profile of air temperature in urban canyons; so, they are not due to specific features of the two Mediterranean cities but are rather inherent limitations of the model. As opposite to the daytime inaccuracies, UWG estimates well the afternoon and night air temperature in both cities. The average monthly UHI intensity is also well estimated by the model: according to the observations, the average UHI intensity in Rome is equal to 1.9 °C in August and 1.1 °C in January, while the model estimates 2.0 °C and 1.0 °C, respectively. In Barcelona, the average monthly UHI intensity is equal to 0.6 °C in July and 1.5 °C in January while the model estimates 1 °C.

Considering all the results above, the average model error is in line with previous validations in Basel, Switzerland, and in Toulouse, France [74,80], which confirms its ability to capture the average trend of urban air temperature also in the Mediterranean climate. UWG estimations can thus effectively improve the accuracy of building energy simulations for the urban context, because the average trend of urban temperature is well captured by the model. Conversely, the model is not suitable to assess specific urban microclimate at the street level, where temperature gradients should be carefully assessed.

### 3.2 UHI intensity variability in the Mediterranean urban context

The graphs in figure 7 represent the variability of UHI intensity resulting from the parametric analysis performed with UWG. The length of the black bars indicates the maximum variability of the monthly average UHI intensity in January and August determined by the maximum and minimum value of each variable, as defined in table 4. The UHI variability is between 0 °C to more than 2.4 °C, depending on the season and the parameter considered.

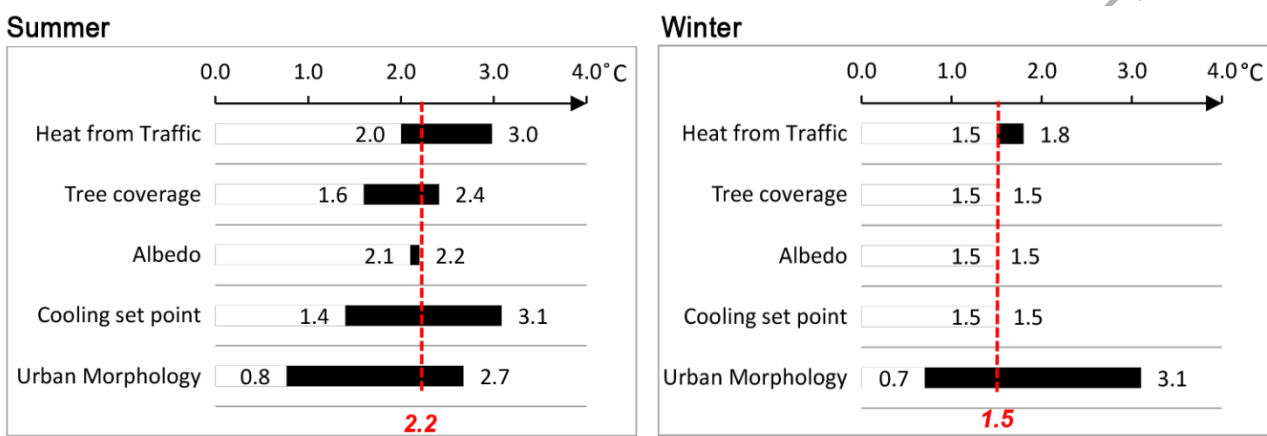


*Figure 7: Variability of the monthly average UHI intensity during August (left) and January (right) in the Mediterranean urban context in relation to the variability of 5 fundamental variables of UHI intensity. The dotted vertical line represents the average UHI intensity in each season, corresponding to the baseline model. For details about the calculation of the parameters see the Appendix A. - (2 column fitting image)*

The results indicate a hierarchy of importance of the impact of the five variables analysed on the average UHI intensity. The most important variable is urban morphology, which can determine substantial variations of the UHI intensity in both seasons (figure 7). In August, the average monthly UHI intensity calculated with the baseline model for the reference context is equal to 2.2°C and the daily maximum UHI intensity equal to 4.6 °C (during night-time at 00:00). The parametric analysis shows that the variability of urban morphology which characterises the two Mediterranean cities can decrease the average UHI intensity to 0.8 °C or increase it up to 2.7 °C; the daily maximum intensity can also increase up to 5.6 °C in the worst scenario. In January, according to the baseline model, the average UHI intensity is equal to 1.5 °C and the daily maximum UHI intensity is 2.7°C, always occurring during night-time. In this season, urban morphology can determine a variability of the average UHI intensity between 0.7 °C and 3.1 °C and a daily maximum UHI intensity up to 5.2 °C; this means that urban morphology has an impact on UHI intensity up to 442% in winter and to 337% in summer.

According to the results of the parametric analysis, another key parameter of UHI intensity is the anthropogenic heat, both from air conditioning systems and traffic. Anthropogenic heat from cooling systems is relevant only in summer. The use of air conditioning with low cooling set point temperatures may cause an increase of the average UHI intensity up to 1.7 °C in comparison to the absence of air conditioning use in the

buildings; the use of air conditioning with the lowest cooling set point (22°C) also determined the maximum daily UHI intensity among all the scenarios, equal to 6.4 °C. The excessive use of air conditioning systems can thus determine a relative change of about 220% of the UHI intensity in summer. This result is in line with the findings from other studies on the impact of the increase in use of air conditioning systems on urban temperature [99,100].

The anthropogenic heat released from traffic is the third significant factor of the summer UHI; considering maximum and minimum traffic conditions, the UHI variability is between 2°C and 3 °C in summer; for the highest value of heat from traffic ( $30 \text{ W/m}^2$ ), the daily maximum UHI intensity reaches up to 6.1 °C. However, this result is probably a bit overestimated, since UWG assumes that the heat released from traffic is constant during the day, while the maximum value used in this analysis corresponds to the peak traffic hours (see Appendix A). This variable has, however, an appreciable effect also during wintertime compared to other, causing an increase of the average UHI intensity of 0.3 °C.

The variability of tree coverage and surface albedo across the cities affected much less both the average and the daily maximum UHI intensity in summer and resulted definitely negligible on the winter UHI intensity. This outcome may be explained in view of the facts that: 1) the range of variability of these variables is smaller than others, so their potential impact on the UHI intensity is decreased and 2) some of the "causes" of the UHI are significantly more important than others.

Actually, the values of surfaces albedo and tree coverage are quite similar among the 10 urban textures analysed here. The tree coverage varies between a minimum of 5% to a maximum of 28% of the total site area, determining a variability of the summer UHI intensity between 1.6 °C and 2.4 °C; for the least favourable value (5%), the daily maximum UHI intensity reaches 5 °C, which is less than the one determined by the alike values of urban morphology or anthropogenic heat. The fact that tree coverage is less influential on the UHI intensity is consistent with other urban studies [1,35,101]. Similarly, the variability of albedo of walls, roads and roof within the two urban areas area is not so significant to determine appreciable effects on the UHI intensity at the local scale. Even though this variable has a huge potential on reducing surface temperature, an increase of albedo of an entire neighbourhood would be needed to appreciate significant effects at the local scale.

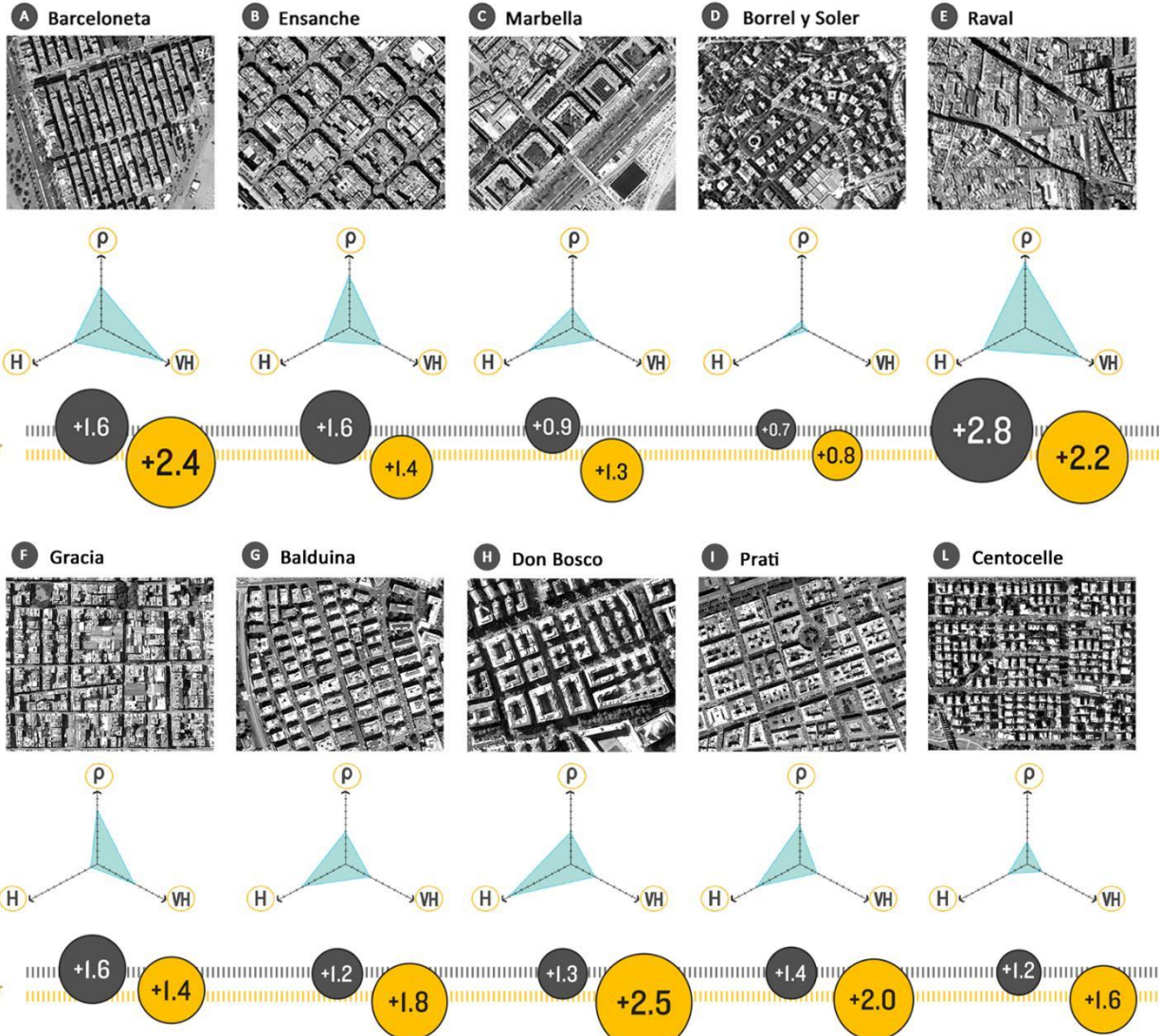


Figure 8 Samples of urban textures of Rome and Barcelona used as study cases for the parametric analysis of UHI intensity in the Mediterranean context. The radar graphs represent the standardized values of the three morphological parameters: Average Building height (Hbld), 'Site coverage ratio' (Purb) and 'Façade-to-site ratio' (VHurb). The numbers in the circles indicates the average UHI intensity during January (grey) and July (yellow). - (2 column fitting image)

Table 5: values of the three morphology parameters for the 10 urban textures

	A	B	C	D	E	F	G	H	I	L
	Barceloneta	Ensanche	Mar Bella	Borrel y Soler	Raval	Gracia	Balduina	Don Bosco	Prati	Centocelle
Purb	0,52	0,62	0,33	0,20	0,80	0,64	0,43	0,43	0,49	0,34
VHurb	2,23	0,71	0,92	0,63	1,38	0,89	1,28	1,68	1,43	1,35
Hbld	16,50	15,95	19,52	15,00	19,50	11,60	19,50	25,50	19,50	14,67

It has also to be highlighted that Rome and Barcelona are characterised by dense and compact urban textures (table 5), which play an important role in modifying the actual albedo through urban geometry. These results in fact suggest that the most important causes of the UHI in the Mediterranean context are the radiative and mechanic phenomena that take place in the urban canyons. Since anthropogenic heat from buildings and traffic also depend on urban density and morphology, this variable appears to be the most important determinant of UHI intensity in the Mediterranean context.

Figure 8 shows the variability of UHI intensity in July (summer) and January (winter) on the 10 represented morphologies. The highest UHI intensity is estimated for the morphology of Raval, during wintertime. The maximum summer UHI intensities are instead calculated for Don Bosco and Barceloneta. The results also suggest that the climatic behaviour of the same urban morphology can be different in summer and in winter, as clearly shown by the results for Don Bosco, Barceloneta and Prati. Therefore, while it is clear that denser urban structures perform worse in terms of UHI intensity, the relationship between the three characteristics of urban morphology and the climatic performance of the texture is not at all intuitive.

### 3.3 Quantitative relationships between urban morphology parameters and UHI intensity

Multiple linear regression analysis applied to a wide set of simulation results (180 UWG runs) allowed deriving the two following relationships between the three morphological parameters and the summer and winter UHI intensity:

$$UHI_W = 0.92 X1(\rho_{urb}), +0.34 X2(VH_{urb}) + 0.05 X3(h_{bld}) \quad (1)$$

$$UHI_S = 0.42 X1(\rho_{urb}), +0.90 X2(VH_{urb}) + 0.32 X3(h_{bld}) \quad (2)$$

In the two relationships, the dependent variables  $UHI_W$  and  $UHI_S$  are the standardized values of the average UHI intensity in winter and summer and the independent variables  $X1(\rho_{urb})$ ,  $X2(VH_{urb})$  and  $X3(h_{bld})$  are the standardized values of ‘Site coverage ratio’, ‘Façade-to-site ratio’ and ‘Average building height’. The statistical significance of the results is very high for both relationships (table 7) as well as the fit of the regression model, with adjusted  $R^2$  equal to 0.9 and 0.8, respectively.

Table 6: standardized values of the three morphology parameters for the 10 urban textures

Original variables			Standardized Variables		
purb	VHurb	Hbld	X1 (purb)	X2 (VHurb)	X3 (Hbld)
0.10	0.50	12	-1.33631	-1.33631	-1.26491
0.25	1.00	15	-0.80178	-0.80178	-0.63246
0.40	1.50	18	-0.26726	-0.26726	0
0.55	2.00	21	0.267261	0.267261	0.632456
0.70	2.50	24	0.801784	0.801784	1.264911
0.85	3.00		1.336306	1.336306	
Average	0.475	1.750	18.000	0.000	0.000
St. Deviation	0.280624	0.935414	4.743416	1	1

Table 7: Regression statistics and significance

Regression Statistics	$UHI_S$	$UHI_W$
Multiple R	0.9497	0.8972
R Square	0.9020	0.8050
Adjusted R Square	0.9004	0.8017
Standard Error	0.3155	0.4452
Observations	180	180

**Significance F**

<b>Coefficients</b>	1.58874E-88	3.07E-62
<b>Intercept</b>	1.17222E-15	-1.7E-15
<b>Variable X 1</b>	0.4187	0.9194
<b>Variable X 2</b>	0.8962	0.3364
<b>Variable X 3</b>	0.3191	0.0468

One of the most interesting implication of this analysis is the fact that the relationship between urban morphology and UHI intensity varies over the year. The coefficients in equation (1) and (2) highlight in fact the different importance of the three morphological features on the climatic performance of the texture during winter season and summer season. This is interesting because the impact of UHI intensity on the building energy performance is opposite during the two seasons: during summer time it is obviously detrimental, but during winter time it allows a decrease of energy consumptions [22].

Equation (1) shows that during wintertime the most important parameter for UHI intensity is the site coverage ratio, because its standardized value has the highest coefficient (0.92) in the equation. Secondary for importance, there is the façade-to-site ratio, with a coefficient equal to 0.34. The average building height is instead much less important on the UHI in winter, being its coefficient equal to 0.05. Therefore, this indicates that an increase of site coverage ratio determines a significant increase of the average UHI intensity in the urban texture during wintertime, while variations of the façade-to-site ratio or of the average building height are expected to have much less impact on winter urban temperature.

Equation (2) shows instead a different hierarchy of importance of the three parameters on the summer UHI intensity; in this case, the most important parameter is the façade-to-site ratio, which is multiplied to the maximum coefficient (0.90), followed by the site coverage ratio (0.42) and the average building height (0.32). Therefore, the relative weight of the three parameters on the climate performance of urban textures in summer is more balanced than in winter. However, according to the equation, the amount of building facades in the urban area is the most impacting variable on the UHI intensity in the hot season.

The two equations explain the variability of the summer and winter climate performance of the ten case studies in light of their morphological features (figure 8). The maximum winter UHI intensity was in fact predicted for Raval, which is the texture with the highest value of site coverage ratio among the ten. Furthermore, all the textures with high values of site coverage ratio showed a high UHI intensity during wintertime rather than summer time (e.g. Ensanche, Raval and Gracia). Conversely, the importance of the façade-to- site ratio is clear looking at the result for Barceloneta, whose building typology with high amount of facades is detrimental on the summer UHI intensity. The equations also explain why Don Bosco is the urban texture with the worst climatic performance among the ten case studies, having the highest summer UHI

intensity and one of the lowest winter UHI intensity; this behaviour is caused by the fact that the value of the site coverage ratio is not very high, and so the corresponding winter UHI intensity, while the high values of average building height and the façade-to-site ratio determine a high summer UHI intensity.

### **3.2.1. Climatic performance of the urban textures: graphic tools**

The results discussed so far also allowed to create some graphic tools (figure 9) to compare the climatic performance of urban textures in summer and winter based on their morphological features. These can be used for any other urban texture of Rome and Barcelona whose morphological parameters are known and for similar urban areas with the limitations reported in paragraph 4.2.

The graphic tools are designed to identify the climatic performance of an urban texture based on its location on the corresponding graph; there are 5 different graphs corresponding to different average buildings heights: 12 m, 15 m, 18 m ,21 m and 24 m (the 5 graphs can be found in figure 9 and Appendix b). Each band of colour represents an increase of the average UHI intensity of about 0.2 °C.

The use of the graphs to compare the climatic performance of three of the previous case studies is reported as an example. Ensanche, Borrel y Soler and Centocelle have similar average building height around 15m, so their performance can be analysed on the same graph. The comparison highlights a good climatic performance of Ensanche, which has a low UHI intensity during both seasons. It also highlights the poor climatic performance of Centocelle, which has a higher UHI intensity in summer than in winter; the morphology of Centocelle determines a summer UHI intensity around 1.8-2.0 °C, which is even higher than the one of Ensanche (1.4-1.6 °C), despite this latter is a much denser urban texture in terms of built volume. This happens because the morphology of Centocelle is composed of small buildings arranged on a dense network of roads, which results in an high amount of façade surfaces (i.e. façade-to-site ratio) in comparison to the buildings footprint.

From the graphs, it can also be deduced that for values of the site coverage ratio below 0.55, the UHI intensity in winter is rather low, regardless of the values of the other parameters. Above that threshold, any further increases of the site coverage ratio would instead result in a significant increase of the UHI intensity.

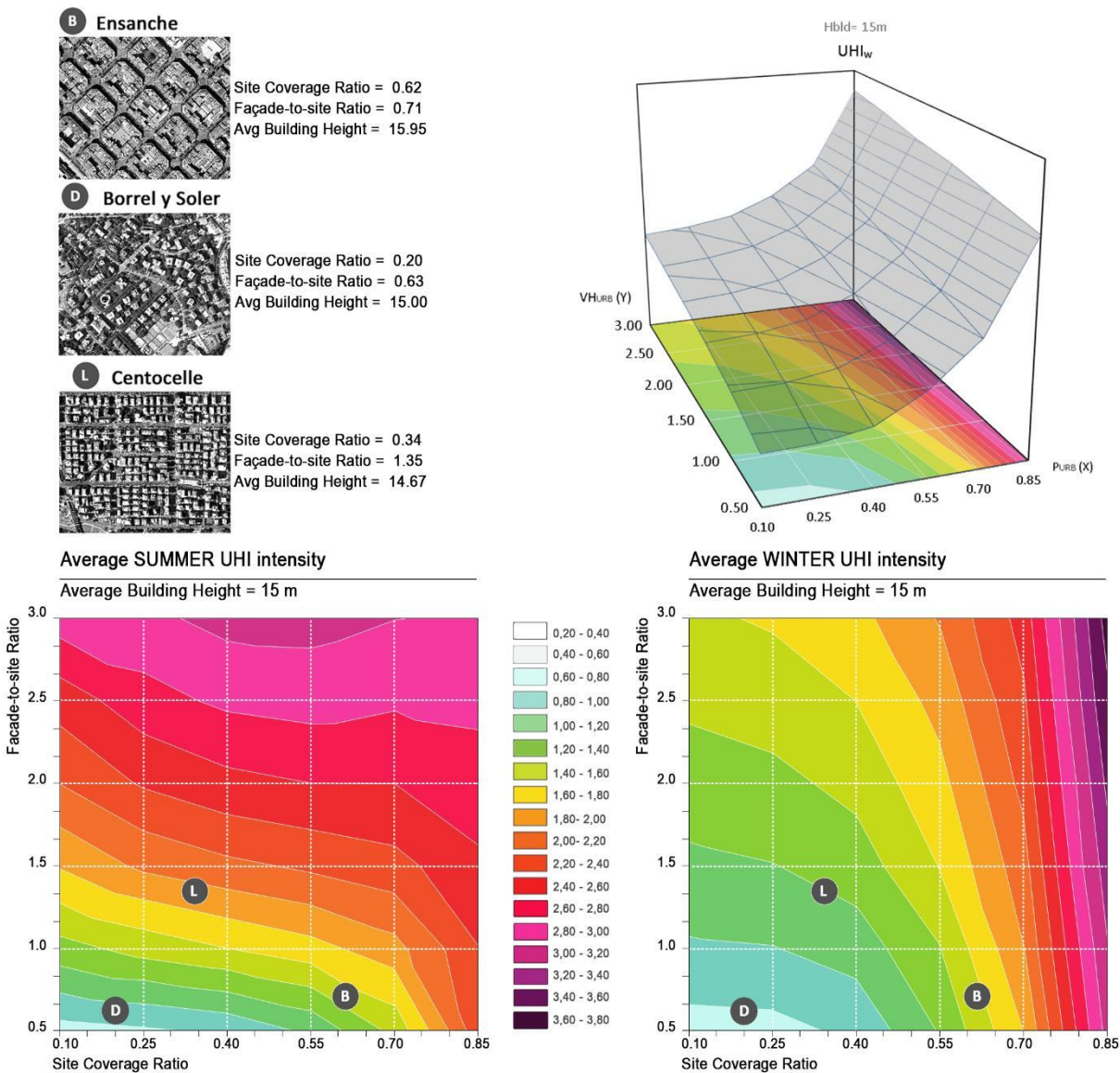


Figure 9 The graphical tools can be used to compare the average summer and winter UHI intensities of different urban textures, knowing the values of Average Building height' ( $h_{bld}$ ), 'Site coverage ratio' ( $p_{urb}$ ) and 'Façade-to-site ratio' ( $V_{Hurb}$ ). The graphs have been obtained analysing UWG simulation results for different average building heights in a three-dimensional Cartesian coordinate system (in the upper right side of the picture), whose axes were the Site Coverage ratio (x-axis), the Façade-to-site ratio (y-axis) and the Average UHI intensity (z-axis). The projection of the surface on the horizontal X-Y plane gave the corresponding 2D graphs, as those reported in the bottom of the picture. An example on how to use them is provided using the values of the three textures represented in the upper left side of the picture. - (2 column fitting image)

#### 4. Discussion

##### 4.1. Impact of 'Vertical Density' and 'Horizontal density' on climate performance of urban textures

The significance of the results presented lies in the identification of a seasonal variability of the impact of urban morphology on UHI intensity in a Mediterranean urban context. Two types of density differently affect the trend of urban temperature in the hot and the cold season, namely the 'Horizontal density' and the 'Vertical density'.

Horizontal density is synonymous of urban compactness, namely it indicates how close the buildings are in an urban area; so, the horizontal density increases proportionally to the value of the site coverage ratio (figure 10).

'Vertical density' indicates the quantity of vertical surfaces (façades) in an urban area, which is obviously dependant on the average building height but also on the building typology. In fact, the same volume can be built using building typologies with different ratios of envelope area to floor area [102], such as for example detached houses or apartment blocks. Therefore, depending on the prevalent building typology, urban textures with the same average coverage ratio and building height, but different façade-to-site ratios exist (figure 10). That is why the 'Vertical density' is proportional to both the Average building height and the Façade-to-site ratio of an urban texture.

In light of the results, an increase of horizontal density of urban textures determines an increase of the UHI intensity in winter, while an increase of vertical density entails an increase of UHI intensity in summer. This can be explained considering the variability of solar radiation and anthropogenic heat generation during the year in the Mediterranean context and their interaction with urban geometry.

At these latitudes (around 41.5° N), solar radiation and solar altitude increase significantly in summer compared to winter. This entails that some of the causes of UHI effect such as the multiple reflections of solar radiation in urban canyons during daytime [28,50] and the decrease of long-wave radiation loss during night time [28,46] have their maximum impact in summer. Higher solar altitudes and intensity mean in fact a higher absorption of solar radiation during the day which is dissipated slowly during night time due to reduced values of SVF in urban canyons; in summer, these are probably the most important cause of UHI intensity in the Mediterranean context. This explains why the summer UHI intensity is maximum in urban textures with high values of 'vertical density', since their building typologies with high amounts of facades optimize solar radiation absorption and allows for heat storage during the day than in turn provokes higher temperatures at night time. The impact of façade density on radiation absorption and trapping had been already highlighted in computational and experimental studies on urban albedo [103,104].

The same phenomena occur also in winter, but they are probably less important because solar radiation intensity and altitude is much lower than in summer. As opposite to this, the anthropogenic heat from buildings is higher in winter than in summer, because space heating is present in almost all the buildings, while space cooling is much less common in residential buildings in the Mediterranean context. Therefore, the anthropogenic heat generated by buildings is probably the most important cause of UHI intensity in winter in the Mediterranean context. This is sure for higher latitudes such as in London, where it was found

that the heat from anthropogenic sources was much higher than the one from solar radiation in winter [105]. In compact urban textures, the heat released from buildings is most likely to remain within the canopy layer, because wind velocity is greatly reduced in the canyon and so the exchange rate with the upper layer of atmosphere. So, the closer are the buildings (or the higher it is the horizontal density) and the lower is the turbulent transport of heat out of the canyon and, consequently, the maximum is the difference of temperature with respect to rural unobstructed environments.

These results thus indicate that to improve the climatic performance of urban textures in the Mediterranean climate, building height should be reduced and urban compactness should be increased. This would lead to a mitigation of UHI in summer while taking advantage of the beneficial effect of higher urban temperatures in winter.

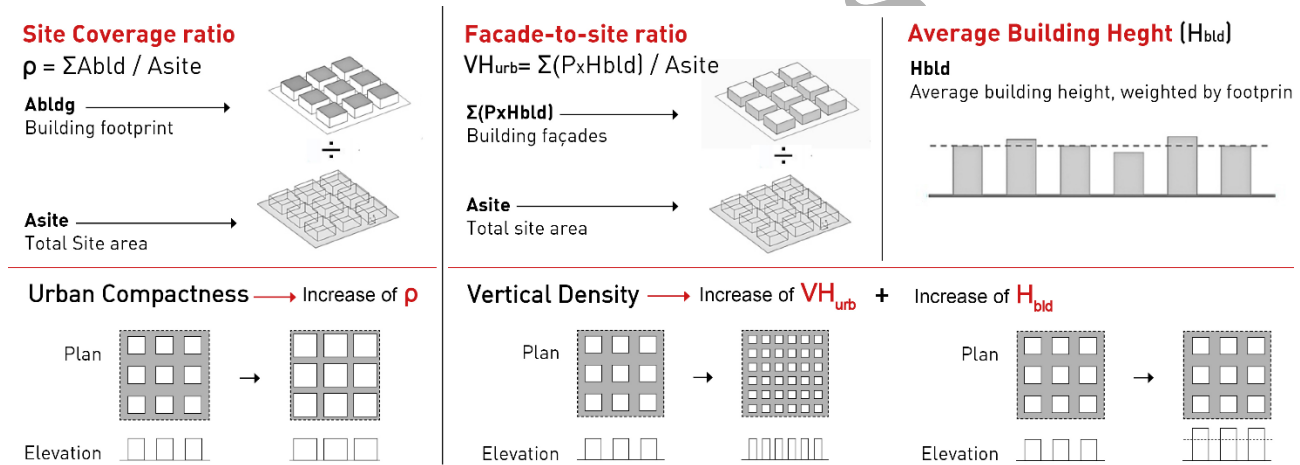


Figure 10 morphological meaning of horizontal density and vertical density - (2 column fitting image)

The three morphological parameters used by UWG could be used also to improve the classification of built types for the LCZ classification, overcoming the limitations of describing urban morphology by adimensional parameters such as the SVF or the canyon aspect ratio. It is clear that also the three UWG parameters still provide a very simplified representation of urban morphology. However, they catch the most important features of urban form influencing air temperature in the urban canopy layer - the horizontal density and the vertical density - and could be used to provide more accurate estimations of the seasonal variability of UHI intensity at the local scale. The validity of these findings is also strengthened by the results of a recent study [103] showing that the net radiation balance calculated over detailed geometrical models of real urban textures and over equivalent simplified urban layouts are very similar if the simplified models have the same site-coverage ratio and facade-to-site ratio of the real urban textures.

#### 4.2. Limitations and range of applicability of the tools

The relationships identified between morphology parameters and UHI intensity are statistically-based and thus to be considered valid only when the same boundary conditions apply in terms of climate (i.e. Csa in Koppen-Geiger classification), location (similar latitude and proximity to the sea) and average values of anthropogenic heat from traffic and buildings, vegetation coverage and albedo of surfaces. In any case, the climatic performance calculated with the graphic tools should be interpreted as a relative assessment rather than an absolute value of UHI intensity; the accuracy of the absolute estimation depends on the conformity of the other parameters to the values set in the baseline model. In particular, considering the results of the parametric analysis, a range of variability of the climatic performance is expected if the values of tree coverage and anthropogenic heat from traffic and buildings are significantly different from the values set in the baseline model. Furthermore, the calculations have been performed using the latitude of Rome as reference (Lat 41.47N); therefore, the validity of results for other regions with Mediterranean climate in the world such as California, central Chile and Australia should be further investigated, as well as for other cities in the Mediterranean basin characterised by a different macroclimate in terms of precipitation and wind speed.

The validity of results is also subject to the limitations of UWG model, which is a bulk model designed to estimate an average value of air temperature in urban canyons; the results can be considered reliable for homogeneous urban areas, where climate is not influenced by the presence water bodies, vast parks or orographic conditions, which are not considered in the calculation [74,106]. The tools provided can be used to estimate the variability of the average UHI intensity at the local scale across a Mediterranean city [57] but should not be used for an estimations of the UHI intensity at the city scale neither to performed detailed microclimate studies of specific urban spaces.

The average summer and winter UHI intensities calculated with the tools can be used to adjust the weather files for urban building energy modelling, as shown in previous works [22,46,107]. However, also the modification of wind field, shadows and radiant environment in the urban texture should be carefully considered when estimating building energy demand in urban contexts, otherwise the impact of UHI intensity could be overestimated, as shown in a recently published work on the topic [19]. Finally, urban morphology parametrisation adopted by the model has also some limitations. UWG uses the three morphological parameters to obtain the characteristics of the average urban canyon and perform the calculations under the following hypothesis: 1) all the urban canyons in the area are the same, 2) the urban canyon is considered of infinite length and 3) the urban canyons have an average orientation. This simplification entails some errors in the calculation of the solar gains; Cantelli et al. [108] provided an accurate analysis of this topic,

highlighting that the error varies in relation to the value of the site coverage ratio and the main orientation of the urban fabric. These finding can be used to improve further the geometrical representation adopted by UWG in future works.

## 5. Conclusions

This study used the climate model UWG to provide tools for comparative analysis of the climatic performance of urban textures in a Mediterranean urban context.

UWG was validated using actual temperature observations from urban weather stations in Rome and Barcelona. The model performed a very good estimate of the UHI intensity during night-time; during daytime, it tended to over-estimates the temperature observed at the roof level and to under-estimate temperature at street level. In spite of these inaccuracies on the daytime temperature, the model is deemed suitable to improve the accuracy of climate data for building energy modelling, because it calculates reasonably well the average increase of urban temperature.

A base-line model for the Mediterranean context was set identifying the average value of the most significant urban variables over a sample of 10 urban textures of Rome and Barcelona. The range of variability of the three morphology parameters used by UWG were also identified. These were used to perform a representative set of simulations with UWG, so as to analyse the variability of UHI intensity using multiple regression analysis.

Two distinct relationships were identified between the three morphological parameters and the UHI intensity in summer and winter. Based on these results, some graphical tools were created to perform fast evaluations of the climatic performance of urban textures based on their morphology.

The results suggested that urban heat island in winter is higher in compact urban textures with site coverage ratios above 0.5, where buildings are very close one to another. This kind of layout contributes to urban temperature increase because it enhances the storage of anthropogenic heat from buildings and vehicles within the canopy. Conversely, during summer time, urban heat island is higher in urban textures with high 'vertical density', which are characterised by building types that optimise solar absorption on the facades during daytime and then tend to remain warmer also at night, because the heat losses through long-wave radiation are reduced by the low values of sky view factor.

The novelty of this study hence consists in the identification of a parameterisation system of urban geometry able to capture the three-dimensional features of the urban texture that affect the climatic performance and to quantify the expected UHI intensity during winter and summer. The tools provided allow for rapid

evaluations of the average UHI intensity in different urban textures, just using the three morphological parameters, easily obtainable from GIS data.

These results should be of great interest to planners and urban designers to deeper the understanding of the relationships between urban morphology and climate performance. Quantitative results also provided new insights on how to improve the climatic performance of urban textures controlling key morphological features such as height of buildings, depth of buildings plan and urban layouts that could allow enhancing the winter UHI intensity and decreasing the summer one, providing a good behaviour during the whole year.

The implementation of tools capable of handling the complexity of urban phenomena, with a degree of approximation suitable for the application to the construction industry, is necessary to support the work of professionals involved in the challenge of reducing the energetic and environmental impact of the built environment.

In the attempt of improving the sustainability of urban systems, the opportunity of densifying existing urban areas may have contrasting outcomes in terms of energy and environmental impacts, which are not always taken into account at the urban planning stage. The present study aims at giving an original contribution in this field, encouraging the integration of urban climatology knowledge into the practice of urban planning and design, by providing professionals and planners with adequate quantitative analysis tools to understand complex energy phenomena that take place at an urban scale.

## conflict of interests statement

We declare that the study is an original research carried out as part of a joint PhD programme between Sapienza University of Rome and Polytechnic University of Catalunya. It has not been previously published, neither it is under consideration for publication elsewhere. If accepted, it will not be published elsewhere in the same form, in English or in any other language, including electronically without the written consent of the copyright-holder.

All the authors approve the publication of the article and declare not to have any conflicts of interest to disclose.

## **Appendix A**

The computation of the three parameters of ‘Urban Morphology’ was performed over CAD models of the 10 urban textures, built from detailed GIS data of the buildings’ footprints and heights. The tree coverage was computed on aerial images derived from Google Earth®.

The maximum variability of anthropogenic heat from traffic was calculated according to the formulation of Sailor and Lu [109], considering statistics of the ‘daily vehicle distance per capita’ and population density variability for Spanish and Italian cities [110]. The maximum value corresponds to peak hour in the densest urban context. The average urban value has been assumed equal to  $8 \text{ W/m}^2$  based on literature [74,90].

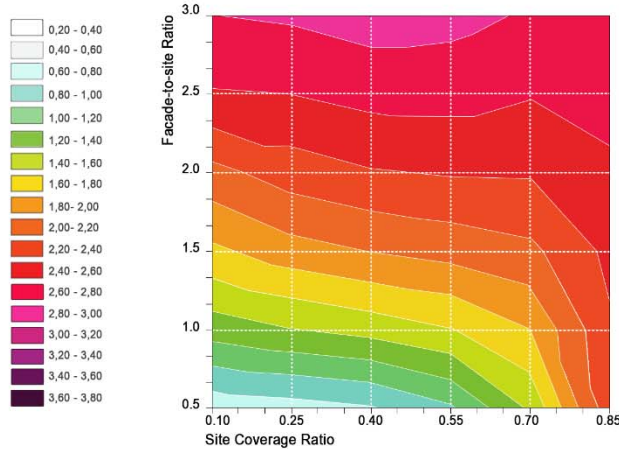
The average maximum and minimum value of surfaces’ albedo was assessed on the 10 urban textures through site surveys and analysis of google street maps images.

The definition of cooling setpoint variability is much harder, since it would require the acquisition of information from all the buildings within the urban area; the value of this parameter is also likely to be different within the same building. In the model, it is used to calculate the average building cooling consumption and proportionally the waste heat released in the urban canyon. For this study, an ‘a priori’ variability has been fixed, ranging from very low values ( $22^\circ\text{C}$ ) to a very high value ( $35^\circ$ ), which indicates the absence of mechanical cooling. Further details on the methodology and results of the parametric analysis of UHI intensity for the Mediterranean climate can be also found in a previous work of Salvati et al. [89].

## Appendix B

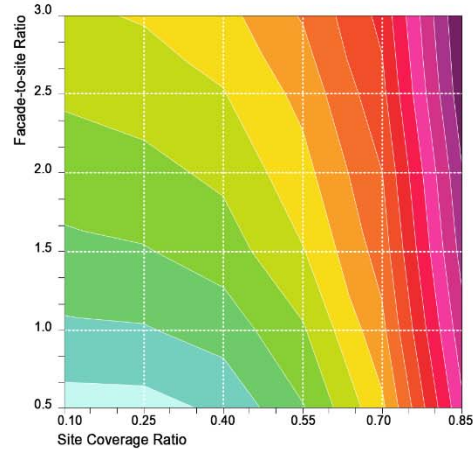
Average SUMMER UHI intensity

Average Building Height = 12 m



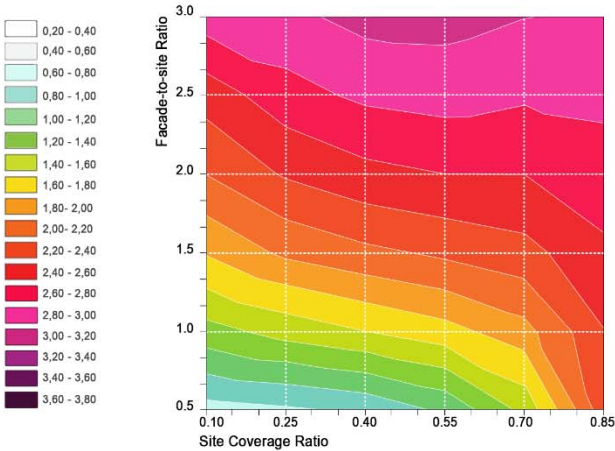
Average WINTER UHI intensity

Average Building Height = 12 m



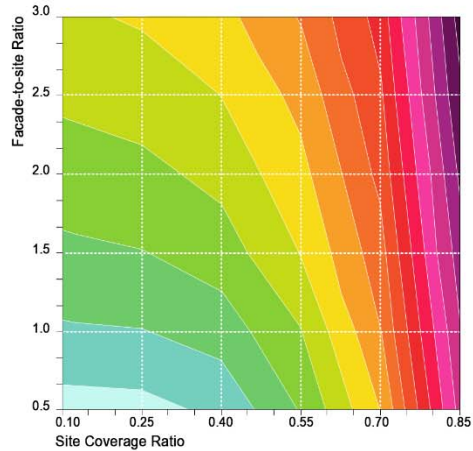
Average SUMMER UHI intensity

Average Building Height = 15 m



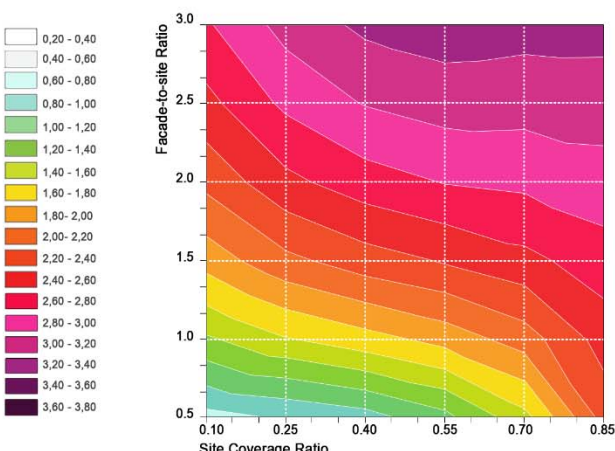
Average WINTER UHI intensity

Average Building Height = 15 m



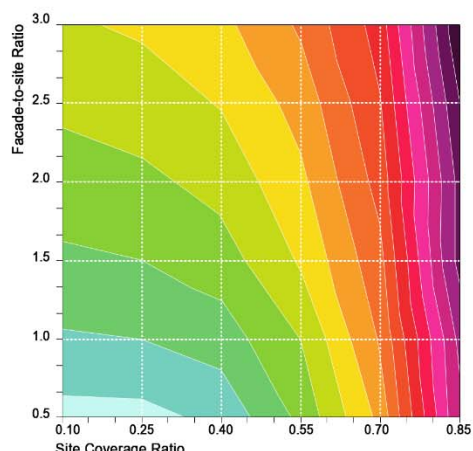
Average SUMMER UHI intensity

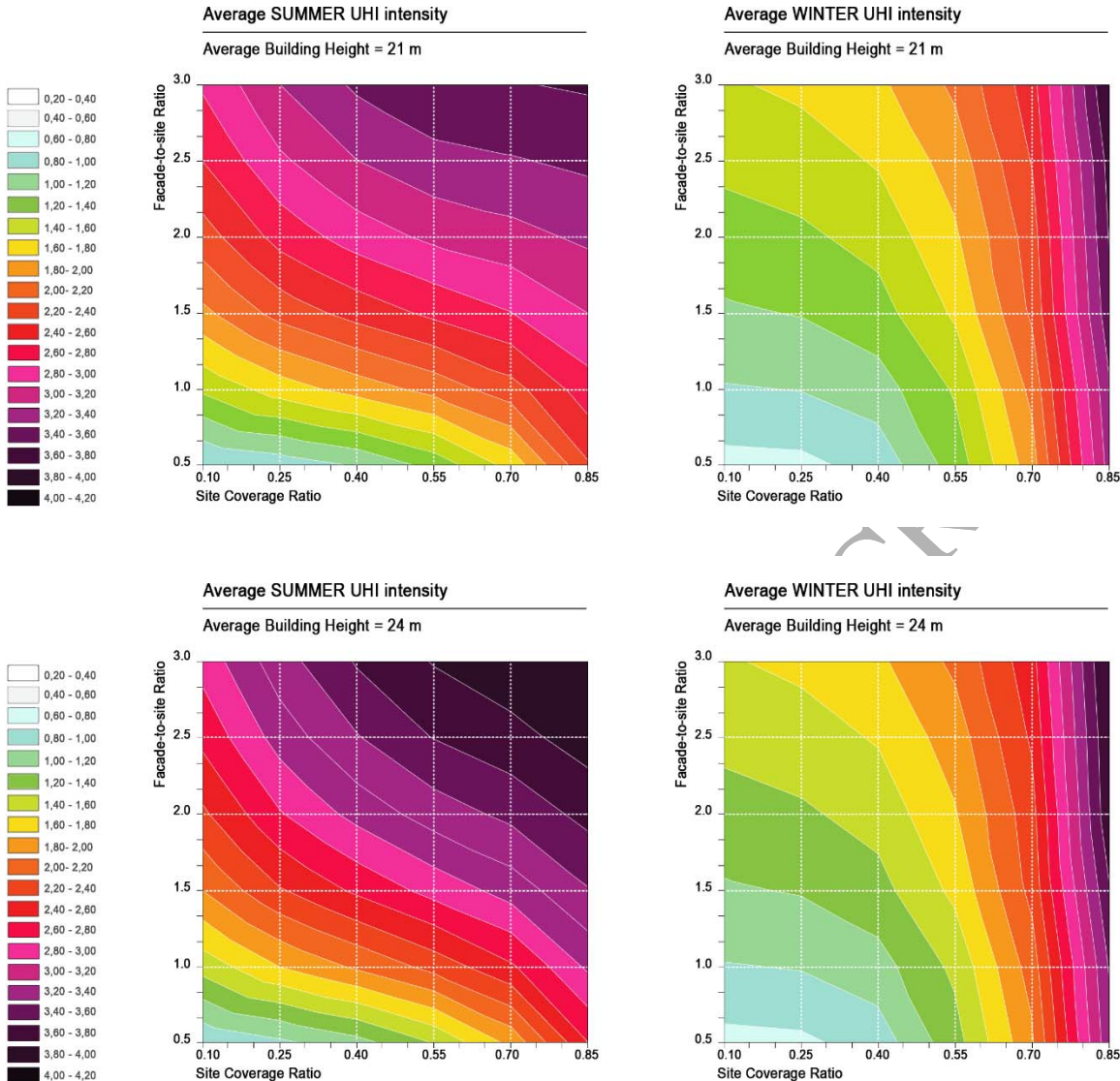
Average Building Height = 18 m



Average WINTER UHI intensity

Average Building Height = 18 m





## References

- [1] L. Inostroza, M. Palme, F. De La Barrera, A heat vulnerability index: Spatial patterns of exposure, sensitivity and adaptive capacity for Santiago de Chile, *PLoS One.* 11 (2016) 1–26. doi:10.1371/journal.pone.0162464.
- [2] C. Mora, B. Dousset, I.R. Caldwell, F.E. Powell, R.C. Geronimo, C.R. Bielecki, C.W.W. Counsell, B.S. Dietrich, E.T. Johnston, L. V Louis, M.P. Lucas, M.M. McKenzie, A.G. Shea, H. Tseng, T.W. Giambelluca, L.R. Leon, E. Hawkins, C. Trauernicht, Global risk of deadly heat, *Nat. Clim. Chang.* 7 (2017) 501–506.
- [3] European Environmental Agency, Extreme temperatures and health, (2016). <http://www.eea.europa.eu/data-and-maps/indicators/heat-and-health-1/assessment-1>.

- [4] M. Stefanon, F. Dandrea, P. Drobinski, Heatwave classification over Europe and the Mediterranean region, *Environ. Res. Lett.* 7 (2012). doi:10.1088/1748-9326/7/1/014023.
- [5] European Environment Agency, Climate change, impacts and vulnerability in Europe 2016. An indicator-based report., Publications Office of the European Union, Luxembourg, 2017. doi:10.2800/534806.
- [6] M. Santamouris, On the energy impact of urban heat island and global warming on buildings, *Energy Build.* 82 (2014) 100–113. doi:10.1016/j.enbuild.2014.07.022.
- [7] T. Zachariadis, P. Hadjinicolaou, The effect of climate change on electricity needs – A case study from Mediterranean Europe, *Energy*. 76 (2014) 899–910. doi:10.1016/j.energy.2014.09.001.
- [8] J. Palmer, I. Cooper, Housing Energy Fact File, Dep. Energy Clim. Chang. (2013) 171. doi:URN: 13D/276.
- [9] C.Y. Yi, C. Peng, Correlating cooling energy use with urban microclimate data for projecting future peak cooling energy demands ..., *Sustain. Cities Soc.* 35 (2017) 645–659. doi:10.1016/j.scs.2017.09.016.
- [10] A.G. Touchaei, M. Hosseini, H. Akbari, Energy savings potentials of commercial buildings by urban heat island reduction strategies in Montreal (Canada), *Energy Build.* 110 (2016) 41–48. doi:10.1016/j.enbuild.2015.10.018.
- [11] F. Chen, H. Kusaka, R. Bornstein, J. Ching, C.S.B. Grimmond, S. Grossman-Clarke, T. Loridan, K.W. Manning, A. Martilli, S. Miao, D. Sailor, F.P. Salamanca, H. Taha, M. Tewari, X. Wang, A.A. Wyszogrodzki, C. Zhang, The integrated WRF/urban modelling system: Development, evaluation, and applications to urban environmental problems, *Int. J. Climatol.* 31 (2011) 273–288. doi:10.1002/joc.2158.
- [12] F. Salamanca, A. Martilli, A new Building Energy Model coupled with an Urban Canopy Parameterization for urban climate simulations-part II. Validation with one dimension off-line simulations, *Theor. Appl. Climatol.* 99 (2010) 345–356. doi:10.1007/s00704-009-0143-8.
- [13] H. Akbari, M. Pomerantz, H. Taha, Cool surfaces and shade trees to reduce energy use and improve air quality in urban areas, *Sol. Energy*. 70 (2001) 295–310. doi:10.1016/S0038-092X(00)00089-X.
- [14] J.A. Futcher, T. Kershaw, G. Mills, Urban form and function as building performance parameters, *Build. Environ.* 62 (2013) 112–123. doi:10.1016/j.buildenv.2013.01.021.
- [15] C.F. Reinhart, C. Cerezo Davila, Urban building energy modeling - A review of a nascent field, *Build. Environ.* 97 (2016) 196-202. doi:10.1016/j.buildenv.2015.12.001.

- [16] J. Allegrini, K. Orehounig, G. Mavromatidis, F. Ruesch, V. Dorer, R. Evins, A review of modelling approaches and tools for the simulation of district-scale energy systems, *Renew. Sustain. Energy Rev.* 52 (2015) 1391–1404. doi:10.1016/j.rser.2015.07.123.
- [17] V. Cheng, K. Steemers, Modelling domestic energy consumption at district scale: A tool to support national and local energy policies, *Environ. Model. Softw.* 26 (2011) 1186–1198. doi:10.1016/j.envsoft.2011.04.005.
- [18] P. Remmen, M. Lauster, M. Mans, M. Fuchs, T. Osterhage, D. Müller, TEASER: an open tool for urban energy modelling of building stocks, *J. Build. Perform. Simul.* (2017) 1–15. doi:10.1080/19401493.2016.1283539.
- [19] M. Palme, L. Inostroza, A. Salvati, Technomass and cooling demand in South America: a superlinear relationship?, *Build. Res. Inf.* 46 (2018) 864–880. doi:10.1080/09613218.2018.1483868.
- [20] A. Vartholomaios, A parametric sensitivity analysis of the influence of urban form on domestic energy consumption for heating and cooling in a Mediterranean city, *Sustain. Cities Soc.* 28 (2017) 135–145. doi:10.1016/j.scs.2016.09.006.
- [21] J.A. Futcher, G. Mills, The role of urban form as an energy management parameter, *Energy Policy*. 53 (2013) 218–228. doi:10.1016/j.enpol.2012.10.080.
- [22] A. Salvati, H. Coch, M. Morganti, Effects of urban compactness on the building energy performance in Mediterranean climate, *Energy Procedia. CISBAT* 201 (n.d.).
- [23] C. Ratti, N. Baker, K. Steemers, Energy consumption and urban texture, *Energy Build.* 37 (2005) 762–776. doi:10.1016/j.enbuild.2004.10.010.
- [24] J. Futcher, G. Mills, R. Emmanuel, I. Korolija, Creating sustainable cities one building at a time: Towards an integrated urban design framework, *Cities.* 66 (2017) 63–71. doi:10.1016/j.cities.2017.03.009.
- [25] J. Rodríguez-álvarez, Urban Energy Index for Buildings (UEIB): A new method to evaluate the effect of urban form on buildings' energy demand, *Landsc. Urban Plan.* 148 (2016) 170–187. doi:10.1016/j.landurbplan.2016.01.001.
- [26] J. Allegrini, V. Dorer, J. Carmeliet, Influence of morphologies on the microclimate in urban neighbourhoods, *J. Wind Eng. Ind. Aerodyn.* 144 (2015) 108–117. doi:10.1016/j.jweia.2015.03.024.
- [27] M. Kolokotroni, R. Giridharan, Urban heat island intensity in London: An investigation of the impact of physical characteristics on changes in outdoor air temperature during summer, *Sol. Energy.* 82 (2008) 986–998. doi:10.1016/j.solener.2008.05.004.

- [28] T.R. Oke, Street design and urban canopy layer climate, *Energy Build.* 11 (1988) 103–113. doi:10.1016/0378-7788(88)90026-6.
- [29] M. Ignatius, N.H. Wong, S.K. Jusuf, The significance of using local predicted temperature for cooling load simulation in the tropics, *Energy Build.* 118 (2016) 57–69. doi:10.1016/j.enbuild.2016.02.043.
- [30] T. Houet, G. Pigeon, Mapping urban climate zones and quantifying climate behaviors--an application on Toulouse urban area (France)., *Environ. Pollut.* 159 (2011) 2180–2092. doi:10.1016/j.envpol.2010.12.027.
- [31] M. Silva, Urban Form and Energy Demand: A Review of Energy-relevant Urban Attributes, *J. Planning Literature* 32 (2017) 346-365. doi:10.1177/0885412217706900.
- [32] M.B. Pont, P. Haupt, The Spacemate :Density and the Typomorphology of the Urban Fabric, *Nord. Arkit.* 4 (2005) 55–68.
- [33] V. Dorer, J. Allegrini, Urban Climate and Energy Demand in Buildings. Final Report, (2012). <http://www.bfe.admin.ch/php/modules/enet/streamfile.php?file=000000010715.pdf&name=000000290497>.
- [34] M. Santamouris, Heat Island Research in Europe: The State of the Art, *Adv. Build. Energy Res.* 1 (2007) 123–150. doi:10.1080/17512549.2007.9687272.
- [35] M. Palme, G. Villareses, L. Inostroza, A. Lobato, C. Carrasco, From urban climate to energy consumption. Enhancing building performance simulation by including the urban heat island effect, *Energy Build.* 145 (2017) 107-120. doi:10.1016/j.enbuild.2017.03.069.
- [36] M. Santamouris, N. Papanikolaou, I. Livada, I. Koronakis, C. Georgakis, a Argiriou, D.. Assimakopoulos, On the impact of urban climate on the energy consumption of buildings, *Sol. Energy.* 70 (2001) 201–216. doi:10.1016/S0038-092X(00)00095-5.
- [37] A. Salvati, H. Coch, C. Cecere, Assessing the urban heat island and its energy impact on residential buildings in Mediterranean climate: Barcelona case study, *Energy Build.* 146 (2017) 38–54. doi:10.1016/j.enbuild.2017.04.025.
- [38] V. Bonacquisti, G.R. Casale, S. Palmieri, a M. Siani, A canopy layer model and its application to Rome., *Sci. Total Environ.* 364 (2006) 1–13. doi:10.1016/j.scitotenv.2005.09.097.
- [39] M. Colacino, a. Lavagnini, Evidence of the urban heat island in Rome by climatological analyses, *Arch. Meteorol. Geophys. Bioclimatol. Ser. B.* 31 (1982) 87–97. doi:10.1007/BF02311344.
- [40] M.C. Moreno-Garcia, Intensity and form of the urban heat island in Barcelona, *Int. J. Climatol.* 14 (1994) 705–710. doi:10.1002/joc.3370140609.

- [41] P. Monti, G. Leuzzi, A numerical study of mesoscale airflow and dispersion over coastal complex terrain, *Int. J. Environ. Pollut.* 25 (2005) 239–250. doi:10.1504/IJEP.2005.007670.
- [42] A. Fanchiotti, E. Cornielo, M. Zinzi, Impact of cool materials on urban heat islands and on buildings comfort and energy consumption, in: World Renew. Energy Forum, WREF 2012, Denver, Colorado, 2012. [https://ases.conference-services.net/resources/252/2859/pdf/SOLAR2012\\_0176\\_full paper.pdf](https://ases.conference-services.net/resources/252/2859/pdf/SOLAR2012_0176_full paper.pdf).
- [43] M. Zinzi, E. Carnielo, Impact of urban temperatures on energy performance and thermal comfort in residential buildings. The case of Rome, Italy, *Energy Build.* 157 (2017) 20–29. doi:10.1016/j.enbuild.2017.05.021.
- [44] S. Magli, C. Lodi, L. Lombroso, A. Muscio, S. Teggi, Analysis of the Impact of Urban Heat Island on Building Energy Consumption, *Energy Environ. Eng.* 6 (2015) 91–99. doi:10.1007/s40095-014-0154-9.
- [45] C. Calice, C. Clemente, A. Salvati, M. Palme, L. Inostroza, Urban Heat Island effect on the energy consumption of institutional buildings in Rome, *IOP Conf. Ser. Mater. Sci. Eng.* 245 (2017) 082015. doi:10.1088/issn.1757-899X.
- [46] J. Allegrini, V. Dorer, J. Carmeliet, Influence of the urban microclimate in street canyons on the energy demand for space cooling and heating of buildings, *Energy Build.* 55 (2012) 823–832. doi:10.1016/j.enbuild.2012.10.013.
- [47] M. Kolokotroni, I. Giannitsaris, R. Watkins, The effect of the London urban heat island on building summer cooling demand and night ventilation strategies, *Sol. Energy.* 80 (2006) 383–392. doi:10.1016/j.solener.2005.03.010.
- [48] J.R. Álvarez, Heat Island and Urban Morphology: Observations and analysis from six European cities, *PLEA 2013 Sustain. Archit. a Renew. Futur.* (2013).
- [49] I.D. Stewart, T.R. Oke, Local Climate Zones for Urban Temperature Studies, *Bull. Am. Meteorol. Soc.* 93 (2012) 1879–1900. doi:10.1175/BAMS-D-11-00019.1.
- [50] N.E. Theeuwes, G.J. Steeneveld, R.J. Ronda, B.G. Heusinkveld, L.W. a van Hove, a. a M. Holtslag, Seasonal dependence of the urban heat island on the street canyon aspect ratio, *Q. J. R. Meteorol. Soc.* (2014) 2197–2210. doi:10.1002/qj.2289.
- [51] A. Di Bernardino, P. Monti, G. Leuzzi, G. Querzoli, Water-Channel Study of Flow and Turbulence Past a Two-Dimensional Array of Obstacles, *Boundary-Layer Meteorol.* 155 (2015) 73–85. doi:10.1007/s10546-014-9987-2.
- [52] K. Niachou, I. Livada, M. Santamouris, Experimental study of temperature and airflow distribution

- inside an urban street canyon during hot summer weather conditions. Part II: Airflow analysis, *Build. Environ.* 43 (2008) 1393–1403. doi:10.1016/j.buildenv.2007.01.040.
- [53] T.R. Oke, Canyon geometry and the nocturnal urban heat island: Comparison of scale model and field observations, *J. Climatol.* 1 (1981) 237–254. doi:10.1002/joc.3370010304.
- [54] J. Unger, Intra-urban relationship between surface geometry and urban heat island : review and new approach, *Clim. Res.* 27 (2004) 253–264.
- [55] M. Tsitoura, M. Michailidou, T. Tsoutsos, Achieving sustainability through the management of microclimate parameters in Mediterranean urban environments during summer, *Sustain. Cities Soc.* 26 (2016) 48–64. doi:10.1016/j.scs.2016.05.006.
- [56] K. Giannopoulou, M. Santamouris, I. Livada, C. Georgakis, Y. Caouris, The impact of canyon geometry on intra Urban and Urban: Suburban night temperature differences under warm weather conditions, *Pure Appl. Geophys.* 167 (2010) 1433–1449. doi:10.1007/s00024-010-0099-8.
- [57] T.R. Oke, Towards better scientific communication in urban climate, *Theor. Appl. Climatol.* 84 (2005) 179–190. doi:10.1007/s00704-005-0153-0.
- [58] B. Bechtel, P.J. Alexander, J. Böhner, J. Ching, O. Conrad, Mapping Local Climate Zones for a Worldwide Database of the Form and Function of Cities, *Geo-Information.* 4 (2015) 199–219. doi:10.3390/ijgi4010199.
- [59] P.J. Alexander, G. Mills, Local Climate Classification and Dublin's Urban Heat Island, *Atmosphere* 5 (2014) 755–774. doi:10.3390/atmos5040755.
- [60] Y. Zheng, C. Ren, Y. Xu, R. Wang, J. Ho, K. Lau, E. Ng, GIS-based mapping of Local Climate Zone in the high-density city of Hong Kong, *Urban Clim.* 24 (2017) 419-448. doi:10.1016/j.uclim.2017.05.008.
- [61] S. Jige, F. Dutt, E. Woodworth, Y. Yamagata, P.P. Yang, Local Climate Zone Mapping for Energy Resilience : A Fine- grained and 3D Approach, *Energy Procedia.* 105 (2017) 3777–3783. doi:10.1016/j.egypro.2017.03.883.
- [62] C.S.B. Grimmond, M. Blackett, M.J. Best, J.-J. Baik, S.E. Belcher, J. Beringer, S.I. Bohnenstengel, I. Calmet, F. Chen, a. Coutts, a. Dandou, K. Fortuniak, M.L. Gouvea, R. Hamdi, M. Hendry, M. Kanda, T. Kawai, Y. Kawamoto, H. Kondo, E.S. Krayenhoff, S.-H. Lee, T. Lorianan, a. Martilli, V. Masson, S. Miao, K. Oleson, R. Ooka, G. Pigeon, a. Porson, Y.-H. Ryu, F. Salamanca, G.J. Steeneveld, M. Tombrou, J. a. Voogt, D.T. Young, N. Zhang, Initial results from Phase 2 of the international urban energy balance model comparison, *Int. J. Climatol.* 31 (2011) 244-272. doi:10.1002/joc.2227.

- [63] C.S.B. Grimmond, M. Blackett, M.J. Best, J. Barlow, J.J. Baik, S.E. Belcher, S.I. Bohnenstengel, I. Calmet, F. Chen, a. Dandou, K. Fortuniak, M.L. Gouvea, R. Hamdi, M. Hendry, T. Kawai, Y. Kawamoto, H. Kondo, E.S. Krayenhoff, S.H. Lee, T. Lorian, a. Martilli, V. Masson, S. Miao, K. Oleson, G. Pigeon, a. Porson, Y.H. Ryu, F. Salamanca, L. Shashua-Bar, G.J. Steeneveld, M. Tombrou, J. Voogt, D. Young, N. Zhang, The international urban energy balance models comparison project: First results from phase 1, *J. Appl. Meteorol. Climatol.* 49 (2010) 1268–1292. doi:10.1175/2010JAMC2354.1.
- [64] T.R. Oke, Boundary layer climates, 2nd ed, Taylor & Francis, London, 1987.
- [65] M. White, An Urban Form Experiment on Urban Heat Island Effect in High Density Area, *Procedia Eng.* 169 (2016) 166–174. doi:10.1016/j.proeng.2016.10.020.
- [66] D. Alobaydi, M.A. Bakarman, B. Obeidat, The Impact of Urban Form Configuration on the Urban Heat Island: The Case Study of Baghdad , Iraq, *Procedia Eng.* 145 (2016) 820–827. doi:10.1016/j.proeng.2016.04.107.
- [67] W. Wang, Y. Xu, E. Ng, Large-eddy simulations of pedestrian-level ventilation for assessing a satellite-based approach to urban geometry generation, *Graph. Models.* 95 (2018) 29–41. doi:10.1016/j.gmod.2017.06.003.
- [68] P. Moonen, T. Defraeye, V. Dorer, B. Blocken, J. Carmeliet, Urban Physics: Effect of the microclimate on comfort, health and energy demand, *Front. Archit. Res.* 1 (2012) 197–228. doi:10.1016/j foar.2012.05.002.
- [69] D. Mauree, S. Cocco, J. Kaempf, J-L Scartezzini, Multi-scale modelling to evaluate building energy consumption at the neighbourhood scale, *Pls One* 12 (2017)e0183437. doi:10.5281/zenodo.847291.Funding.
- [70] S. Gracik, M. Heidarnejad, J. Liu, J. Srebric, Effect of urban neighborhoods on the performance of building cooling systems, *Build. Environ.* 90 (2015) 15–29. doi:10.1016/j.buildenv.2015.02.037.
- [71] J. Bouyer, C. Inard, M. Musy, Microclimatic coupling as a solution to improve building energy simulation in an urban context, *Energy Build.* 43 (2011) 1549–1559. doi:10.1016/j.enbuild.2011.02.010.
- [72] F. Salamanca, A. Krpo, A. Martilli, A. Clappier, A new building energy model coupled with an urban canopy parameterization for urban climate simulations—part I. formulation, verification, and sensitivity analysis of the model, *Theor. Appl. Climatol.* 99 (2009) 331–344. doi:10.1007/s00704-009-0142-9.
- [73] M. Barbason, S. Reiter, Coupling building energy simulation and computational fluid dynamics:

- Application to a two-storey house in a temperate climate, *Build. Environ.* 75 (2014) 30–39. doi:10.1016/j.buildenv.2014.01.012.
- [74] B. Bueno, L. Norford, J. Hidalgo, G. Pigeon, The urban weather generator, *J. Build. Perform. Simul.* 6 (2013) 269–281. doi:10.1080/19401493.2012.718797.
- [75] V. Masson, A physically-based scheme for the urban energy budget in atmospheric models, *Boundary-Layer Meteorol.* 94 (2000) 357–397. doi:10.1023/A:1002463829265.
- [76] B. Bueno, L. Norford, G. Pigeon, R. Britter, Combining a Detailed Building Energy Model with a Physically-Based Urban Canopy Model, *Boundary-Layer Meteorol.* 140 (2011) 471–489. doi:10.1007/s10546-011-9620-6.
- [77] G. Pigeon, K. Zibouche, B. Bueno, J. Le Bras, V. Masson, Improving the capabilities of the Town Energy Balance model with up-to-date building energy simulation algorithms: an application to a set of representative buildings in Paris, *Energy Build.* 76 (2014) 1–14. doi:10.1016/j.enbuild.2013.10.038.
- [78] N. Shishegar, Street Design and Urban Microclimate: Analyzing the Effects of Street Geometry and Orientation on Airflow and Solar Access in Urban Canyons, *J. Clean Energy Technol.* 1 (2013) 52–56. doi:10.7763/JOCET.2013.V1.13.
- [79] J. Mao, J.H. Yang, A. Afshari, L.K. Norford, Global sensitivity analysis of an urban microclimate system under uncertainty: Design and case study, *Build. Environ.* 124 (2017) 153–170. doi:10.1016/j.buildenv.2017.08.011.
- [80] B. Bueno, M. Roth, L. Norford, R. Li, Computationally efficient prediction of canopy level urban air temperature at the neighbourhood scale, *Urban Clim.* 9 (2014) 35–53. doi:10.1016/j.uclim.2014.05.005.
- [81] I. Petenko, G. Mastrantonio, A. Viola, S. Argentini, L. Coniglio, P. Monti, G. Leuzzi, Local Circulation Diurnal Patterns and Their Relationship with Large-Scale Flows in a Coastal Area of the Tyrrhenian Sea, *Boundary-Layer Meteorol.* 139 (2011) 353–366. doi:10.1007/s10546-010-9577-x. [82] G. Leuzzi, P. Monti, 'Breeze analysis By Mast and Sodar Measurements', *Nuovo Cim. C* (1997) 343–359.
- [83] A. Pelliccioni, P. Monti, G. Leuzzi, Wind-speed profile and roughness sublayer depth modelling in urban boundary layers, *Boundary-Layer Meteorol.* 160 (2016) 225–248. doi:10.1007/s10546-016-0141-1.
- [84] A. Redaño, J. Cruz, J. Lorente, Main features of the Sea-Breeze in Barcelona, *Meteorol. Atmos. Phys.* 46 (1991) 175–179.

- [85] Weather Underground, Ciampino Airport Weather Data, (2017).  
[https://www.wunderground.com/history/airport/LIRA/2017/10/13/DailyHistory.html?cm\\_ven=localwx\\_history](https://www.wunderground.com/history/airport/LIRA/2017/10/13/DailyHistory.html?cm_ven=localwx_history)
- [86] Weather Underground, El Prat Airport Weather Data, (2017).  
[https://www.wunderground.com/history/airport/LEBL/2017/10/13/DailyHistory.html?cm\\_ven=localwx\\_history](https://www.wunderground.com/history/airport/LEBL/2017/10/13/DailyHistory.html?cm_ven=localwx_history).
- [87] T.R. Oke, Initial guidance to obtain representative meteorological observations at urban sites, WMO/TD. 1250 (2006).
- [88] T.R. Oke, I.D. Stewart, Local climate zone for urban temperature studies, in: Bull. Amer. Meteor. Soc., 92 (2012) 1879–1900.
- [89] A. Salvati, M. Palme, L. Inostroza, Key Parameters for Urban Heat Island Assessment in A Mediterranean Context: A Sensitivity Analysis Using the Urban Weather Generator Model, in: IOP Conf. Ser. Mater. Sci. Eng. 245 (2017) 82055. doi:10.1088/1757-899X/245/8/082055.
- [90] G. Pigeon, D. Legain, P. Durand, V. Masson, Anthropogenic heat release in an old European agglomeration (Toulouse, France), Int. J. Climatol. 27 (2007) 1969–1981. doi:10.1002/joc.1530.
- [91] P. Zangheri, R. Armani, M. Pietrobon, L. Pagliano, M. Fernandez Boneta, A. Müller, Heating and cooling energy demand and loads for building types in different countries of the EU, 2014. doi:[https://www.google.se/search?q=vienna&rlz=1C1CHBF\\_enSE732SE732&oq=vienna&aqs=chrome..69i57j0l5.290j0j7&sourceid=chrome&ie=UTF-8#q=vienna](https://www.google.se/search?q=vienna&rlz=1C1CHBF_enSE732SE732&oq=vienna&aqs=chrome..69i57j0l5.290j0j7&sourceid=chrome&ie=UTF-8#q=vienna).
- [92] L. Gartland, Heat Islands: Understanding and Mitigating Heat in Urban Areas, London, 2008.
- [93] M. Morganti, SUSTAINABLE DENSITY: Form, Built Environment, Energy, PhD,UPC, SAPIENZA, 2013.
- [94] M. Morganti, H. Coch, C. Cecere, The effect of urban obstruction in Mediterranean climates: built form typology, density and energy, Archit. City Environ. 19 (2012) 13–26.
- [95] H. Saaroni, E. Ben-Dor, A. Bitan, O. Potchter, Spatial distribution and microscale characteristics of the urban heat island in Tel-Aviv, Israel, Landsc. Urban Plan. 48 (2000) 1–18. doi:10.1016/S0169-2046(99)00075-4.
- [96] C. Georgakis, M. Santamouris, Experimental investigation of air flow and temperature distribution in deep urban canyons for natural ventilation purposes, Energy Build. 38 (2006) 367–376. doi:10.1016/j.enbuild.2005.07.009.
- [97] B. Offerle, I. Eliasson, CBS Grimmond, Surface heating in relation to air temperature , wind and

- turbulence in an urban street canyon, *Boundary-Layer Meteorol.* 122 (2007) 273–292. doi:10.1007/s10546-006-9099-8.
- [98] M.W. Rotach, Profiles of turbulence statistics in and above an urban street canyon, *Atmos. Environ.* 29 (1995) 1473–1486. doi:10.1016/1352-2310(95)00084-C.
- [99] F. Salamanca, M. Georgescu, A. Mahalov, M. Moustaqui, M. Wang, Anthropogenic heating of the urban environment due to air conditioning, *J. Geophys. Res. Atmos.* 119 (2014) 5949–5965. doi:10.1002/2013JD021225.Received.
- [100] C. De Munck, G. Pigeon, V. Masson, F. Meunier, P. Bousquet, B. Tréméac, M. Merchat, P. Poeuf, C. Marchadier, How much can air conditioning increase air temperatures for a city like Paris, France?, *Int. J. Climatol.* 33 (2013) 210–227. doi:10.1002/joc.3415.
- [101] E. Ng, L. Chen, Y. Wang, C. Yuan, A study on the cooling effects of greening in a high-density city : An experience from Hong Kong, *Build. Environ.* 47 (2012) 256–271. doi:10.1016/j.buildenv.2011.07.014.
- [102] K. Steemers, Energy and the city: density, buildings and transport, *Energy Build.* 35 (2003) 3–14. doi:10.1016/S0378-7788(02)00075-0.
- [103] D. Groleau, P.G. Mestayer, Urban Morphology Influence on Urban Albedo: A Revisit with the Solene Model, *Boundary-Layer Meteorol.* 147 (2013) 301–327. doi:10.1007/s10546-012-9786-6.
- [104] M. Aida, Urban albedo as a function of the urban structure - A model experiment, *Boundary-Layer Meteorology* 23 (1982) 4:405–413.
- [105] I.G. Hamilton, M. Davies, P. Steadman, A. Stone, I. Ridley, S. Evans, The significance of the anthropogenic heat emissions of London's buildings: A comparison against captured shortwave solar radiation, *Build. Environ.* 44 (2009) 807–817. doi:10.1016/j.buildenv.2008.05.024.
- [106] A. Salvati, H. Coch, C. Cecere, Urban Heat Island Prediction in the Mediterranean Context: an evaluation of the urban weather generator model, *ACE Archit. City Environ. = Arquit. Ciudad Y Entorno.* 11 (2016) 135–156. doi:10.5821/ace.11.32.4836.
- [107] A. Salvati, H. Coch, C. Cecere, Urban Morphology and Energy Performance : the direct and indirect contribution in Mediterranean Climate, in: M. Cucinella, G. Pentella, A. Fagnani, L. D'Ambrosio (Eds.), *PLEA2015 Archit. (R)Evolution - 31st Int. PLEA Conf.*, Bologna, Italy, 2015.
- [108] A. Cantelli, P. Monti, G. Leuzzi, Numerical study of the urban geometrical representation impact in a surface energy budget model, *Environ. Fluid Mech.* 15 (2015) 251–273. doi:10.1007/s10652-013-9309-0.

- [109] D.J. Sailor, L. Lu, A top – down methodology for developing diurnal and seasonal anthropogenic heating profiles for urban areas, *Atmos. Environ.* 38 (2004) 2737–2748.  
doi:10.1016/j.atmosenv.2004.01.034.
- [110] European Commission, Analysis of National Travel Statistics in Europe, 2013. doi:10.2788/59474.

ACCEPTED MANUSCRIPT